UNIVERSITY OF CALIFORNIA SAN DIEGO

The Roles of Beclin1 and Beclin2 in Autophagy and Mitophagy

A dissertation submitted in partial satisfaction of the requirements
for the degree Doctor of Philosophy

in

Biology

by

Eileen Gonzalez

Committee in charge:

Professor Åsa Gustafsson, Chair
Professor Gulcin Pekkurnaz, Co-Chair
Professor Randy Hampton
Professor Andrew McCullouch
Professor Sonya Neal

2022

The Dissertation of Eileen Gonzalez is approved, and it is acceptable in quality and form for publication on microfilm and electronically.

University of California San Diego
2022

DEDICATION

It is a privilege to be loved.

I dedicate this dissertation to my friends and family who have truly loved me.

Words will never be able to capture my immense gratitude.

TABLE OF CONTENTS

TABLE OF CONTENTS (continued)

LIST OF ABBREVIATIONS

Ad-	Adenovirus
αMHC	α-myosin heavy chain
ANOVA	Analysis of variance
Atg	Autophagy
Atg14L	Autophagy Related 14
ATP	Adenosine triphosphate
Baf A1	Bafilomycin A1
BAX/BAK	BCL2-associated X protein (BAX)/BCL2-antagonistic/killer (BAK)
BCL2	B-cell CLL/lymphoma 2
Beclin1 cKO	Tamoxifen-inducible Beclin1$^{f/f}$ mice
CVD	Cardiovascular disease
DMEM	Dulbecco's modified eagle medium
DMSO	Dimethyl sulfoxide
DTT	Dithiothreitol
EDTA	Ethylenediaminetetraacetic acid
EGTA	Ethylene glycol-bis(β-aminoethyl ether)-N,N,N',N'-tetraacetic acid
ER	Endoplasmic reticulum
FBS	Fetal bovine serum
FCCP	Carbonyl cyanide-4-(trifluoromethoxy)phenylhydrazone
GAPDH	Glyceraldehyde-3-phosphate dehydrogenase
GFP	Green fluorescent protein
IMM	Inner mitochondrial membrane

LC3	Microtubule-associated protein 1 light chain 3
MEF	Mouse embryonic fibroblast
MOI	Multiplicity of infection
mtDNA	Mitochondrial DNA
OCR	Oxygen consumption rate
OMM	Outer mitochondrial membrane
OXPHOS	Oxidative phosphorylation
PBS	Phosphate buffered saline
PCR	Polymerase chain reaction
pH	Potential of hydrogen
PINK1	PTEN-induced putative kinase 1
qPCR	Quantitative polymerase chain reaction
ROS	Reactive oxygen species
SDS-PAGE	Sodium dodecyl sulfate-polyacrylamide gel electrophoresis
S.E.M.	Standard error of the mean
siRNA	Small interfering ribonucleic acid
TOM	Translocase of the outer mitochondrial membrane
TIM23	Mitochondrial Import Inner Membrane Translocase subunit
UVRAG	UV radiation resistance associated gene
VPS	Vacuolar protein sorting
WT	Wild type

LIST OF FIGURES

LIST OF FIGURES (continued)

ACKNOWLEDGEMENTS

I would like to acknowledge Dr. Asa, Gustafsson for her guidance and support during my time in her lab. I sincerely value and appreciate my time in her lab.

I would also like to acknowledge Monica Jeung, my master's student mentee, who dedicated so much time and effort to this project. It was a joy to mentor her and watch her grow as a scientist.

Finally, I would like to acknowledge past and present Gustafsson lab members for their comradery in lab through the ups and downs. Special thanks to Nav, Rachel and Wenjing for being inspirational scientists and even better friends.

Parts of Chapter 2, 3, 4 and 5 are in preparation for a manuscript for submission to a journal. Gonzalez, E. R., Jeung, M., Gustafsson, Å. B. The primary author is the lead investigator and author of this manuscript.

VITA

2014	Bachelor of Sciences, Microbiology, California State University, Los Angeles
2022	Doctor of Philosophy, Biology, University of California San Diego

PUBLICATIONS

Gonzalez ER, Jeung M, and Gustafsson ÅB. Elucidating the roles of Beclin1 and Beclin2 in Autophagy and Mitophagy. *Manuscript in preparation*.

Lally NS, Moyzis AG, Gonzalez ER, Diao R, Najor RH, Chi L, and Gustafsson ÅB. Mcl-1 differentially regulates non-selective autophagy and the selective autophagy of damaged mitochondria. *Manuscript in preparation.*

Lampert M[Co-1st], Lally N[Co-1st], Gonzalez ER, Najor R, Diao R, Liang W, Chi L, Manso AM, Yue Z, Adler E, and Gustafsson ÅB. Beclin1-mediated Protein Trafficking is Essential for Cardiac Homeostasis. *Circ Research*. 2021 May. *Under Revision.*

Woodall BP, Orogo AM, Najor RH, Cortez MQ, Moreno ER, Wang H, Divakaruni AS, Murphy AN, and Gustafsson ÅB. Parkin does not prevent accelerated cardiac aging in mitochondrial DNA mutator mice. *JCI Insight*. 2019 Apr. DOI: 10.1172/jci.insight.127713

Hammerling BC, Najor RH, Cortez MQ, Shires SE, Leon LJ, Gonzalez ER, Boassa D, Phan S, Thor A, Jimenez RE, Li H, Kitsis RN, Dorn GW, Sadoshima J, Ellisman MH, and Gustafsson ÅB. A Rab5 endosomal pathway mediates Parkin-dependent mitochondrial clearance. *Nature Communications.* 2017 Jan. DOI: 10.1038/ncomms14050

Orogo AM, Gonzalez ER, Kubli DA, Baptista IL, Ong S-B, Prolla TA, Sussman MA, Murphy AN, Gustafsson, ÅB. Accumulation of Mitochondrial DNA Mutations Disrupts Cardiac Progenitor Cell Function and Reduces Survival. *Journal of Biological Chemistry.* 2015 Sep. DOI10.1074/jbc.M115.649657

Mansor LS, Gonzalez ER, Cole MA, Tyler DJ, Beeson JH, Clarke K, Carr CA, Heather LC. Cardiac Metabolism in a New Rat Model of Type 2 Diabetes Using High-Fat Diet with Low Dose Streptozotocin. *Cardiovascular Diabtetology*. 2013 Sep. DOI: 10.1186/1475-2840-12- 136

Yamazaki KG, Gonzalez ER, Zambon AC. Crosstalk Between the Renin- Angiotensin System and the Advance Glycation End Product Axis in the Heart: Role of the Cardiac Fibroblast. *J Cardiovasc Trans Res*. 2012 Sep. DOI: 10.1007/s12265-012-9405-4

PRESENTATIONS

Oral Presentation at the American Heart Association Basic Cardiovascular Sciences (BCVS) (2019)

Poster Presentation at UCSD Biological Sciences Annual Retreat (2018)

AWARDS

NIH National Institutes of Biomedical Imaging and Bioengineering (NIBIB) T32 Graduate Research Training Grant at UCSD

UCSD 2018 Grad Slam Finalist: annual public speaking competition showcasing my research in a three-minute elevator pitch

ABSTRACT OF THE DISSERTATION

The Roles of Beclin1 and Beclin2 in Autophagy and Mitophagy

by

Eileen Gonzalez

Doctor of Philosophy in Biology

University of California San Diego, 2022

Professor Åsa Gustafsson, Chair

Professor Gulcin Pekkurnaz, Co-Chair

Quality control mechanisms are indispensable to the maintenance of cellular homeostasis. The dependency on these mechanisms changes greatly in response to stress, and dysfunction either in baseline quality control or in stress-dependent pathways is associated with a variety of human diseases. Autophagy is an important cellular quality control mechanism and is responsible for degrading unwanted or damaged cellular

components. Autophagosome formation is initiated by the Class III PI3K complex, comprised of Beclin1, ATG14L, VPS34, and VPS15. In this dissertation, I focus on the role of Beclin1 and its homolog Beclin2 in regulating autophagy. To perform these investigations, I utilized a combination of biochemical and imaging techniques, CRISPR-Cas9 gene editing, and siRNA-mediated knockdown experiments to dissect the role(s) of Beclin1 and/or Beclin2 in autophagy. Our evidence demonstrates that autophagosomes are still formed in the absence of Beclin1 and Beclin2 but to a reduced extent. Furthermore, we provide evidence of a Beclin1-and-Beclin2-independent autophagy pathway.

Additionally, this dissertation explores the role of Beclin1 in the mitochondrial-specific process of autophagy, termed mitophagy. Evaluation of mitophagy revealed that Beclin1, but not Beclin2, plays a role in this process. Specifically, we found that cells lacking Beclin1 had decreased rates of mitochondrial clearance due to reduced targeting of autophagosomes to damaged mitochondria. Overexpression of a Beclin1 phosphorylation resistant mutant in Becn1$^{-/-}$ cells confirmed that the Serine 15 in the unique N-terminus is important for successful targeting of autophagosomes to mitochondria. Beclin1 Serine 15 is a known Ulk1 phosphorylation site and we confirmed a similar targeting defect exists in the absence of Ulk1. Together, these findings provide increased insights into the roles of Beclin1 and Beclin2 in autophagy and mitophagy.

Finally, this dissertation details the development of a new fluorescent reporter for use in in vitro and in vivo experiments assessing mitophagy. Using a series of set criteria, we generated several different constructs and evaluated their effectiveness as mitophagy reporters. Ultimately, we identified a reporter containing a tandem mCherry-pHluorin2

fluorophore that is targeted to the mitochondria and anchored to the inner membrane to be the most effective in assessing mitophagy events. This reporter did not alter mitochondrial morphology, maintained strong fluorescence post-fixation, and labeled mitochondria in autophagolysosomes as only mCherry positive. This reporter allows for improved tracking and quantification of mitophagy and provides a useful tool for researchers studying this essential quality control pathway.

CHAPTER 1: Introduction

1.1 Cellular Quality Control Mechanisms

1.1.1 Autophagy. At baseline, cells are constantly generating and consuming to maintain life, and as a result, are also continuously generating waste. Homeostatic mechanisms are in place to maintain cellular function and viability. Understanding these processes, the molecular players involved, and their importance in cellular homeostasis is imperative to our understanding of cellular biology. Autophagy is an intracellular degradation pathway and an important quality control mechanism in the cell. At baseline, autophagy is responsible for the turnover of cellular components (He et al., 2013). In response to starvation, autophagy is increased to recycle amino acids and fatty acids so that the cells can maintain energy levels (Guo et al., 2016). In response to cellular stress, autophagy is responsible for the removal of damaged protein aggregates and damaged organelles (Dikic & Elazar, 2018).

Autophagy was first observed in yeast by Yoshinori Ohsumi in 1992. Using yeast cells lacking vacuolar degradation enzymes, which enable the cell to degrade unwanted cellular material, his group observed that under starvation conditions many smaller vesicles formed within cells (Nakatogawa et al., 2009; Takeshige et al., 1992). They discerned that cells rely on vacuolar degradation to maintain themselves under starved conditions. Subsequently, key autophagy-related genes (ATG) were identified using the yeast model and with time, many mammalian orthologs have also been identified (Nakatogawa et al., 2009; Tanida et al., 2001).

Since its discovery 30 years ago, our understanding of autophagy, has greatly increased and we are continuing to unravel the intricacies of this process and the

molecular components involved. It is also clear that dysregulation of autophagy is linked to a variety of diseases. For example, excessive activation of autophagy is detrimental in type 2 diabetes (Kanamori et al., 2015), whereas diminished autophagy enhances cardiac dysfunction in anthracycline-induced cardiotoxicity (D. L. Li et al., 2016). Dysregulation of autophagy has also been linked to neurodegenerative diseases, inflammation, and cancer (Kuma et al., 2017; X. H. Liang et al., 1999; Yang et al., 2014). Despite the recognition that the process of cellular degradation and recycling by autophagy is essential for eukaryotic life, there is a great need for further characterization of this process and its dysregulation in human disease.

1.1.2 The Mechanism of Autophagy. Cellular stress can come from a variety of sources, including nutrient deprivation, oxidative stress, or infection. During nutrient deprivation, either AMP-activated protein kinase (AMPK) or mechanistic target of rapamycin-1 (mTORC1) sense the energy status of the cell and signal Unc-51-like kinase 1 (ULK1) to initiate autophagy (Jung et al., 2009, p. 13; Shang et al., 2011). ULK1 forms a complex comprised of ULK1, ATG13, FIP200, and ATG101, which phosphorylates the class III PI3K complex (Lin & Hurley, 2016). The class III PI3K complex includes VPS34 (vacuolar protein sorting), Beclin1, ATG14L, and VPS15, and when activated, this complex generates phosphatidylinositol-3-phosphate (PI3P) at the omegasome structure on the endoplasmic reticulum (ER), leading to the recruitment of additional autophagy proteins (Nascimbeni et al., 2017). Recently, autophagosome formation has been specifically linked to mitochondria-associated membranes (MAMs) where the ER is directly tethered to the mitochondria (Hamasaki et al., 2013; Lewis et al., 2016).

Effector proteins on the autophagosome pre-cursor membrane, also known as the phagophore, recruit the ATG12-ATG5–ATG16L1 complex (Sawa-Makarska et al., 2020). This complex enhances the conjugation reaction that converts microtubule-associated protein light chain 3-I (LC3I) into LC3II, the hallmark of autophagic structures (Mizushima et al., 2001). LC3II interacts with cargo adaptors, such as p62, and the growing phagophore engulfs the cargo to form a double-membraned autophagosome. Maturation of the autophagosome is facilitated by a different PI3K complex, comprised of Beclin1, UV Radiation Resistance Associated (UVRAG), VPS34 and VPS15. The mature autophagosome then fuses with a lysosome for subsequent degradation of its cargo by lysosomal hydrolytic enzymes (Fig. 1.1) (Kang et al., 2011, p. 1; Lamb et al., 2013; Nakatogawa et al., 2009). Recovered nutrients from the breaking down of cargo are transported back to the cytoplasm.

1.2 Mitochondria and Quality Control

1.2.1 Mitochondrial Dynamics. Mitochondria perform several essential functions within the cell, including ATP synthesis, calcium regulation, and cell death control (Galluzzi et al., 2012; Kubli & Gustafsson, 2012). As vital organelles, they have their own dedicated quality control mechanisms that work in tandem to maintain a healthy pool of mitochondria. The coordinated processes of fusion, fission, mitophagy, and biogenesis balance the removal and replacement of unhealthy mitochondria from the cell population (Fig. 1.2) (Pickles et al., 2018). Mitochondrial fusion, the joining of two or more mitochondria, favors higher ATP efficiency, dilutes damaged components, and protects against mitophagy (Chan, 2020; Meyer et al., 2017). In contrast, mitochondria fission

allows for the separation of damaged mitochondrial components (Galluzzi et al., 2012; Meyer et al., 2017). Mitophagy selectively eliminates damaged mitochondria, while biogenesis synthesizes more to ensure constant quality (Chan, 2020; Kubli & Gustafsson, 2012). A careful balance between mitochondrial degradation and synthesis is essential to maintain mitochondrial homeostasis. In fact, dysregulation of any of these quality control processes can negatively affect health. For example, Charcot-Marie Tooth Neuropathy type 2A, a disease that is associated with damage to peripheral nerves, is caused by mutations in the mitochondrial fusion protein mitofusin-2 (MFN2) (Meyer et al., 2017).

1.2.2 Parkin-mediated Mitophagy. Mitochondria can suffer damage from a variety of external and internal factors, including mtDNA mutations, reactive oxygen species (ROS), and toxic chemical exposure (Onishi et al., 2021). Mitophagy is a specialized form of autophagy that selectively sequesters damaged mitochondria into autophagosomes for degradation (Kubli & Gustafsson, 2012). Mitophagy is mediated by the cytosolic E3 ubiquitin ligase Parkin. Parkin-mediated mitophagy is initiated when the mitochondrial membrane potential is compromised, resulting in an accumulation of the mitochondrial PTEN-induced kinase 1 (PINK1) on the outer membrane (Narendra et al., 2010). PINK1 accumulation leads to the recruitment of Parkin, which ubiquitinates outer membrane proteins (Kane et al., 2014). This ubiquitination signals the recruitment of the adaptor protein p62, which subsequently interacts with LC3 on the phagophore (Pankiv et al., 2007). When a mitochondrion is fully engulfed by the autophagosome, it fuses with a lysosome, and the mitochondrion is degraded (Fig. 1.3). Parkin-mediated mitophagy is essential to the maintenance of cellular homeostasis, especially in highly metabolically

active cells. For example, mutations to both PINK and PARKIN have been linked to the neurological illnesses of Parkinson's and Alzheimer's disease (Quinn et al., 2020).

1.3 Beclin1 and Beclin2

1.3.1 Beclin1. Beclin1 is a key component of the class III PI3K complexes involved in autophagosome formation and maturation (McKnight & Zhenyu, 2013; Nakatogawa et al., 2009). Beclin1 was discovered in 1998 as a novel B-cell-lymphoma-2 (Bcl-2)-interacting protein by Beth Levine's group (X. H. Liang et al., 1998). To investigate how Bcl-2 protects against Sindbis viral infection, they performed a yeast two-hybrid screen for Bcl-2 interacting gene products and discovered Beclin1. In follow up studies, the same group established Beclin1 as the first mammalian autophagy gene, identified as the ortholog of the yeast autophagy gene ATG6 ((Yue et al., 2003).

Beclin1 contains a BH3 domain, which classifies it as a Bcl-2-interacting protein as well as a BH3-only protein, which are typically pro-apoptotic (Cao & Klionsky, 2007; Chittenden, 2002; Maiuri, Criollo, et al., 2007, p. 3). Researchers are actively investigating how regulation and competitive disruption of the Beclin1 BH3 domain affects Beclin1 activity; although the isolated BH3 domain of Beclin1 has been seen to induce apoptosis, overexpression of the Beclin1 alone does not affect cell viability (Maiuri, Le Toumelin, et al., 2007). Beclin1 typically exists as a homodimer but can form a heterodimer when in complex with other proteins (X. Li et al., 2012). Beclin1 can interact with UV radiation resistant-associated gene (UVRAG) to regulate vacuolar protein sorting and influence endocytic trafficking in cells (Funderburk et al., 2010; C. Liang et al., 2008).

Global Beclin1 homozygous knockout mice were found to be embryonic lethal, while autophagy-deficient mice develop normally but die shortly after. (Kuma et al., 2017; Yue et al., 2003). This indicates Beclin1 is crucial for embryonic development processes independent of autophagy. Studies using heterozygous Beclin1+/- mice have revealed roles for Beclin1 in tumor proliferation and preventing neurodegeneration (Qu et al., 2003). Beclin1$^{+/-}$ mice also have decreased autophagy in the heart and are more susceptible to myocardial ischemia/reperfusion injury (Matsui et al., 2007), proteotoxicity, sepsis-induced heart damage (Sun et al., 2018), and pressure overload-induced heart failure (Zhu et al., 2007).

Beclin1 is most widely studied for its interaction in the class III PI3K complex, which participates in the initiation of the phagophore membrane in the autophagy process (Nakatogawa et al., 2009). When Bcl-2 interacts with Beclin1 via its BH3-domain, Beclin1 is unable to facilitate the formation of the intact class III PI3K complex, and autophagy initiation is inhibited (Chittenden, 2002, p. 3; Kang et al., 2011; Oberstein et al., 2007, p. 3). A study in mice with a knock-in mutation to Beclin1 that leads to reduced interaction with Bcl-2 also had enhanced baseline autophagy in tissues, reduced development of age-related cardiac hypertrophy, and extended life span (H. Zhu et al., 2007; H. Zhu & He, 2015).

The role of Beclin1 in autophagy is well established; however, there has been much less research addressing if it plays a role in mitophagy. Studies in cells lacking Beclin1 have implicated PINK1 as a regulator of Beclin1's localization to MAMs but molecular evidence for a regulatory role in this process is still limited (Gelmetti et al., 2017). It has been proposed that Beclin1 can regulate mitophagy through its

phosphorylation by Ulk1, the serine/threonine kinase that acts upstream of the Beclin1-PI3-kinase complex in autophagy (Kumar & Shaha, 2018; Russell et al., 2013). Ulk1-deficient cells have impaired mitophagy, suggesting a specific role for Ulk1 in regulating mitophagy (Tian et al., 2015). How Ulk1 selectively regulates mitophagy is actively being investigated and studies have reported various potential mechanisms of regulation. For instance, Vargas et al. reported that the autophagy adaptor protein NDP52 plays a role in recruiting the Ulk1 complex to ubiquitinated cargo (Vargas et al., 2019). However, Mercer et al. has implicated Ulk1 in the phosphorylation of VPS15 to be involved in mitophagy (Mercer et al., 2021). Whether Ulk1 regulates mitophagy directly via Beclin1 has not been investigated.

1.3.2 Beclin2: a homolog of Beclin1. In 2013, He et al. identified Beclin2 as a homolog to Beclin1 (He et al., 2013). Beclin1 and Beclin2 share 57% sequence identity in humans and 44% in mice (He et al., 2013) (Fig. 1.4). Beclin2 has been implicated in autophagy regulation, lysosomal degradation of certain GPCRs, and glucose metabolism (He et al., 2013, p. 2). Beclin2 has also been reported to regulate autophagy by interaction with known binding partners in HeLa cells(He et al., 2013, p. 2). In contrast to Beclin1$^{-/-}$ mice, Beclin2$^{-/-}$ mice were not embryonic lethal. Beclin2$^{-/-}$ mice survived early development at sub-Mendelian rates (4%), suggesting a critical role for Beclin2 in development (He et al., 2013). Since then, research has expanded on the function of Beclin2 in endolysosomal trafficking and degradation of select GPCR's, such as cannabinoid receptors (Kuramoto et al., 2016). More recently, Beclin2 was observed to activate non-canonical autophagy in innate immunity (Dong et al., 2016; M. Zhu et al., 2020).

Although Beclin1 and Beclin2 appear to function in similar pathways, it is still unknown whether they have overlapping and compensatory roles in autophagy. The role of Beclin2 in mitophagy is also unknown. Although He et al. quantified % of cells with less than 10 mitochondria and equated low percent to impaired mitochondrial clearance after stress, a much more in-depth investigation of Beclin2 is clearly needed.

1.4 Approaches to assessing mitophagy in vivo and in vitro

There is clear evidence that functional mitochondrial processes, including mitophagy, are essential to cellular homeostasis. However, tools to monitor and quantify rates of mitophagy are lacking, especially for *in vivo* studies. Existing methods to assess mitophagy have provided important insights but have notable limitations. For example, when mitophagy is assessed biochemically, mitochondrial clearance within the whole population of cells or tissue is assessed. Levels of mitochondrial-associated proteins and mtDNA can also be quantified to provide insight into changes in mitochondria content (Chen et al., 2017). Unfortunately, these methods only lend insight into the process as averaged across a tissue; it does not reflect cell to cell differences. They are also less sensitive and are only useful to detect high levels of mitophagy and assumes that biogenesis is not occurring. The classical approach to measuring mitophagy events in individual cells has been by florescent imaging of colocalization between autophagosomes and mitochondria. However, this approach measures the engulfment of mitochondria and does not reflect the final output step of degradation. Another traditionally used approach has been electron microscopy (EM), to identify mitochondria surrounded by double-membrane autophagic structures. In addition to being very costly,

this technique is also limited since mitochondria undergo severe morphological changes during mitophagy making them difficult to identify by EM as well as difficult to quantify.

In the past decade, various groups have generated fluorescent mitophagy reporters to allow for monitoring of mitophagy both in vitro and in vivo. These reporters also allow the assessment of mitophagy in live cells. However, these reporters have their limitations. The most widely used reporter thus far has been the ratiometric fluorescent probe mt-Keima. The Keima fluorophore was initially used to monitor lysosomal acidity since it was found to be both pH-sensitive and relatively resistant to lysosomal degradation (Bingol et al., 2014; Katayama et al., 2011; N. Sun et al., 2015). Keima has a dual-excitation spectrum and a single emission peak. At a neutral pH, excitation is at 440 nm, which gradually shifts to a 586 nm excitation in an acidic pH. The emission is held constant at 620 nm regardless of the shift in excitation (Katayama et al., 2011). In 2015, the Finkle group targeted Keima to mitochondria (mt-Keima), using a mitochondria-targeting sequence. Since its generation, this reporter has been widely used for both *in vitro* and *in vivo* studies of mitophagy (N. Sun et al., 2015, 2017). The most notable issue with mt-Keima has been in image processing. The bimodal excitation is a unique feature that requires advanced microscopes with specialized filters, limiting use to only those labs with specialized equipment. It is also common to have partial overlap in the emission spectra, which creates concerns for analysis. Additionally, Keima cannot be fixed for imaging since paraformaldehyde quenches the lysosomal acidity and alters the excitation of the reporter. Due to this limitation, all in vivo measurements must be done immediately on freshly harvested and sectioned tissue, which leads to inconsistencies from experiment to experiment and lab to lab.

Another popular mitophagy reporter is mito-QC, which attaches a tandem mCherry–GFP tag to the outer mitochondrial membrane protein FIS1 (residues 101-152)(McWilliams et al., 2016). Since mCherry is relatively resistant to pH change, mitophagy is quantified based on the increase in red-only (mCherry) signal, which happens when the GFP signal is quenched after lysosome fusion. This reporter offers several advantages, including stable fluorescence after fixation and compatibility with more widely used imaging systems (Allen et al., 2013; McWilliams et al., 2019). One advantage of this reporter is the ease of quantification of mitophagy. However, mito-QC is anchored to the outer mitochondrial membrane, and outer membrane proteins are subjected to degradation by the ubiquitin proteasome system (UPS). The UPS is often activated during mitophagy (Karbowski & Youle, 2011; Neutzner et al., 2007).

Another dual-emission reporter is Mt-Rosella, which is the fusion of fluorophores DsRed and GFP with a mitochondrial targeting sequence to ensure its localization to the matrix (Rosado et al., 2008). This reporter has not been as widely used but has benefits similar to mt-QC in fixation ability and ease of use for microscopy (Kobayashi et al., 2020). However, our lab has found that DsRed tagged proteins are more susceptible to aggregation.

While technologies do exist that allow for the tracking and quantification of mitophagy in the cell, there is room for improvement as new fluorophores and technology become available. There is always a need for a reliable up-to-date biosensor that could specifically track mitophagy.

1.5 Rationale and Specific Aims of the Thesis

Although Beclin1 is considered to be critical for autophagy, we observed that autophagy is still intact in cells lacking Beclin1. This suggests that autophagy can be initiated in a Beclin1-independent manner. Beclin2 is a homolog of Beclin1 and has been reported to regulate both autophagy and endosomal-mediated degradation of certain GPCRs. However, few additional studies on Beclin2 have been published since its original discovery in 2013, and potential compensation between Beclin1 and Beclin2 has not been explored.

In addition to its reported role in autophagy, Beclin1 has been implicated in the mitochondrial-specific autophagic process known as mitophagy. We observed that despite intact autophagy, mitophagy is decreased in Beclin1-deficient cells. This suggests that Beclin1 has a specific role in regulating mitophagy but the molecular mechanism underlying the regulation of this process is unknown. Interestingly, the serine-threonine kinase Ulk1 is required for mitophagy and Beclin1 is a known Ulk1 substrate, supporting a putative role for Beclin1 in mitophagy.

I hypothesize that Beclin1 and Beclin2 are involved in the general autophagy pathway, but Beclin1 functions in Parkin-mediated mitophagy.

Aim 1: To investigate the roles of Beclin1 and Beclin2 in autophagy.

Hypothesis: Both Beclin1 and Beclin2 can initiate autophagy in cells, and there exists a compensation mechanism between them to maintain functional autophagy when one homolog is absent.

Aim 2: To investigate how Beclin1 functions in mitophagy.

Hypothesis: The Ulk1-Beclin1 signaling axis regulates mitophagy by promoting autophagosome formation at mitochondria membrane contact sites on damaged mitochondria.

Aim 3: The design and optimization of a new fluorescent mitophagy reporter that will accurately reflect mitophagic events.

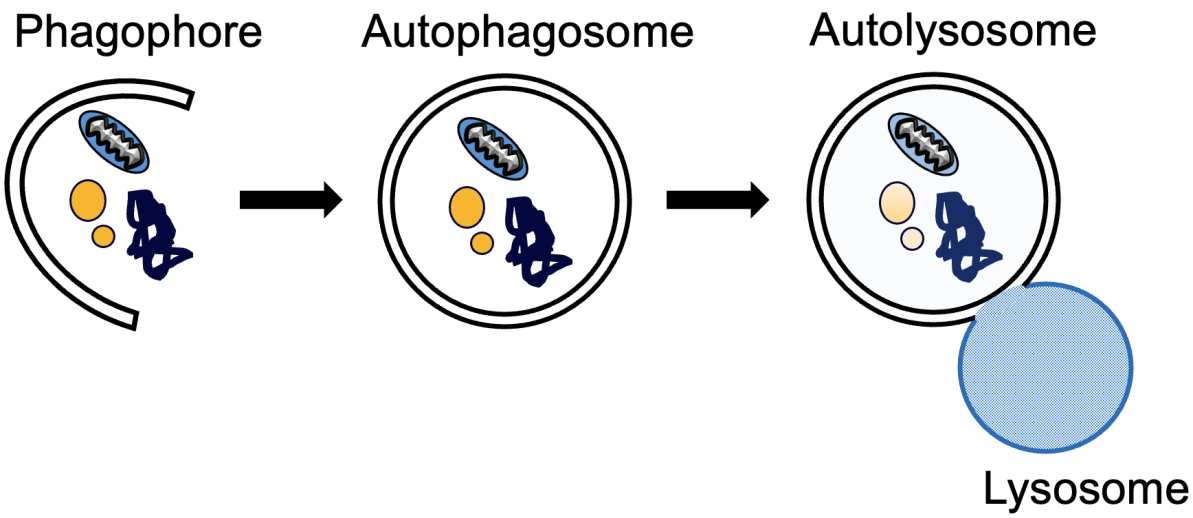

Figure 1.1 Scheme of the autophagy process. The formation of a phagophore is initiated near damaged organelles, protein aggregates, and other cargo labeled for degradation. The phagophore matures into a double membrane structure, known as the autophagosome, that fully encloses around target cargo. The autophagosome then fuses with a lysosome containing hydrolytic enzymes that degrade the cargo.

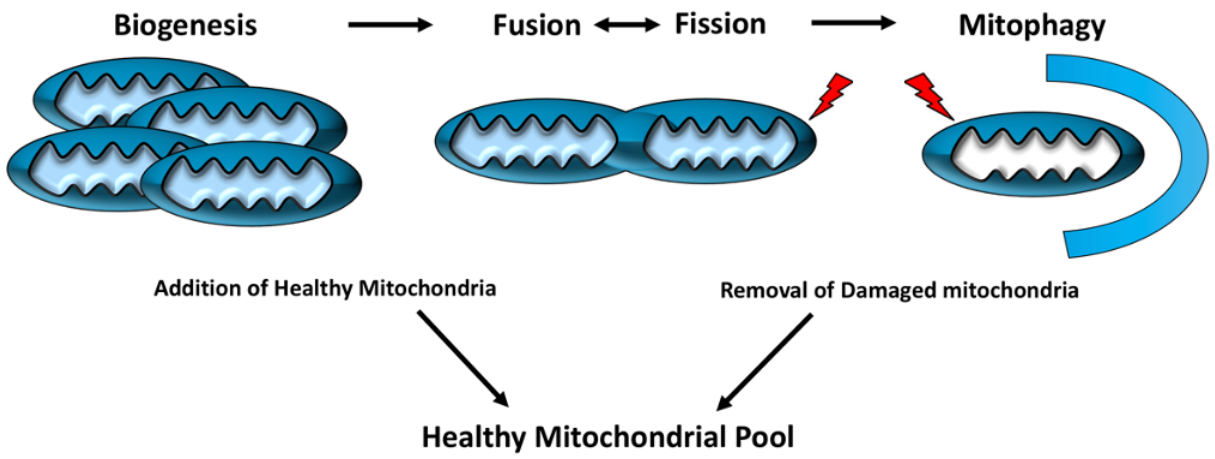

Figure 1.2 Scheme of Mitochondrial Dynamics. Mitochondrial fission, fusion, mitophagy, and biogenesis coordinate to maintain a healthy mitochondrial network in cells. Fusion merges mitochondria together. Fission removes impaired portions of damaged mitochondria. Mitophagy is the selective removal of damaged mitochondria, while biogenesis replenishes these mitochondria.

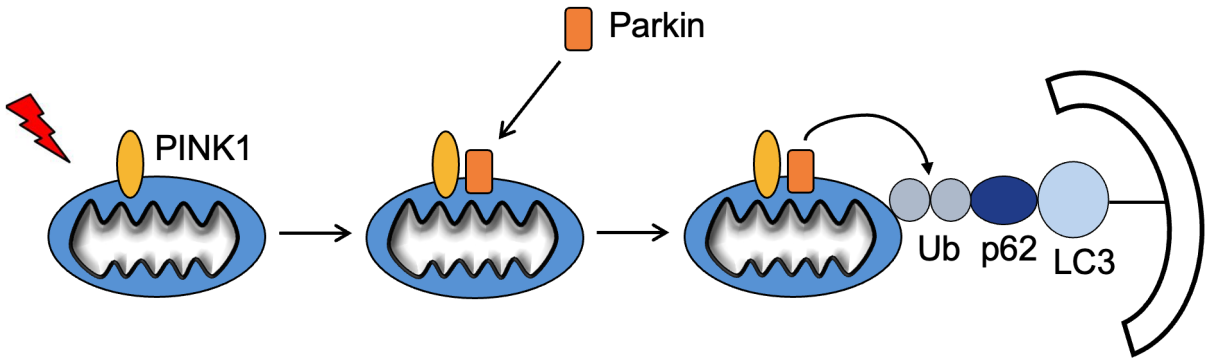

Figure 1.3 Scheme of Parkin-Mediated Mitophagy Pathway. The mitochondrial protein PINK1, accumulates on the outer mitochondrial membrane when membrane potential is lost. The accumulation of PINK1 leads to the recruitment of the E3 ubiquitin ligase, Parkin, which ubiquitinates many substrates on the outer membrane. The ubiquitin recruits p62, the autophagy adaptor protein, which in turn binds to LC3 that links the phagophore to the cargo.

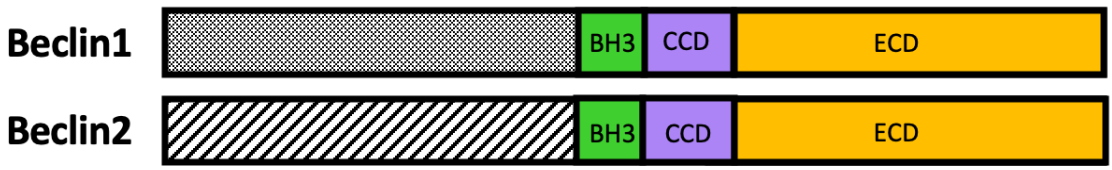

Figure 1.4 Scheme of homologs Beclin1 and Beclin2. Alignment of Beclin1 and Beclin2 sequences. They share identical BH3 domains, the Coil-Coiled domains (CCD), and the evolutionarily conserved domains (ECD), while the N-terminal region is unique.

CHAPTER 2: Experimental Methods and Materials

Cell Lines and Culture Conditions

Cells were cultured in DMEM+ Glutamax media (GIBCO, 10569-044) supplemented with 10% FBS (GIBCO, 16000-044) and 1% antibiotic-antimycotic (GIBCO, 15240-062). Cells were maintained in a 5% CO2 atmosphere at 37ºC. Wildtype (WT) and *Becn1*$^{-/-}$ mouse embryonic fibroblasts (MEFs) were generously gifted by Dr. Zhenyu Yue at the Icahn School of Medicine at Mount Sinai (McKnight et al., 2014). WT and *Ulk1*$^{-/-}$ MEFs were generously provided by Dr. Mondira Kundu (St. Jude's Research Hospital, US) (Kundu 2008). All cell lines routinely tested negative for mycoplasma. Chemicals used include Bafilomycin A1 (Sigma, B1793), Oligomycin (MilliporeSigma, 75351), Antimycin A (MilliporeSigma, A8674), FCCP (MilliporeSigma, C2920), and SBI-0206965 (Millipore Sigma, SML1540).

CRISPR Cas Gene Editing

HeLa cells were generated using the Gene Knockout Kit v2 (Synthego) according to the manufacturer's protocol. In brief, we generated ribonucleoprotein complexes using the kit's sgRNAs and Cas9 proteins in a 9:1 ratio and then nucleofected cell suspensions of WT HeLa cells with these complexes. The provided sgRNAs were a combination of 3 different guides targeting either Beclin1$^{-/-}$ or Beclin2$^{-/-}$. Following transfection, half the cell suspension was plated for clonal expansion and the other half for genomic analysis. 72 hours post-transfection, cells were collected for genomic analysis. We isolated DNA and subjected to Sanger-sequencing for the respective amplicons. Using the ICE v2 CRISPR analysis tool, we expanded single cell populations with favorable knockout scores of 85

and above. Clones were expanded from single cells and gene deletion was validated using a combination of the ICE v2 analysis tool, traditional PCR, and Quantitative PCR.

siRNA Knockdown

Beclin2$^{-/-}$ HeLa cells were transfected with either 20nM negative control siRNA (Qiagen, SI03650318; seq: CAGGGTATCGACGATTACAAA) or 50 nM Beclin1 siRNA (Sigma siRNA ID: SASI_Hs01_00090913), using RNAiMax lipofectamine reagent (Thermo Fisher, 13778) according to the manufacturer's protocol. 72 hours post-transfection, cells were treated with Bafilomycin A1, FCCP, or subjected to starvation and collected for Western blot analysis. Knockdown of Beclin1 was confirmed by Western blot for each experiment.

Adenoviral Infection of Cell Lines

Cells were infected with adenovirus in DMEM+ Glutamax with 2% heat-inactivated serum for 3 hours and then rescued with complete culture media. 24 hours post-infection, cells were treated with either FCCP or OA, and collected for Western blot analysis or fixed for imaging. *Adenoviruses***:** mCherry-Parkin (MOI 50), GFP-LC3 (MOI 150) as previously described. MTS-mCherry-phLuorin2-TM (MOI 50) and flag-Parkin (MOI 50) were generated by the viral core at the University of California, Davis.

Transfections

Cells were transiently transfected with Fugene 6 Transfection Reagent (Promega, E269A) in DMEM+ Glutamax for 6 hours and rescued with culture media. 24 hours following transfection, cells were treated and collected for Western blot analysis or fixed for imaging.

Plasmids: GFP-LC3 (Addgene plasmid 11546), Myc-Parkin (Addgene plasmid 17612), a gift from Ted Dawon, mCherryParkin (Addgene plasmid 23956) was a gift from Richard Youle, pcDNA4-Beclin1-HA, a gift from Qing Zhong (Addgene plasmid 24399) (Sun, 2008).

All custom constructs were designed by the author and generated by Genscript on the pcDNA3.1(+) backbone. Beclin1 phospho-resistant mutants were generated by replacing active residues with alanine residues. Each construct was also HA-tagged at the N-terminus. HA-Beclin1S15A, HA-Beclin1S30A, HA-Beclin1T57A, HA-Beclin1S90A, and HA-Beclin1S93A. HA-Beclin2 was created with the Beclin2 human sequence and the addition of an HA-tag at the N-terminus. The splitGFP-MAM reporter was generated in two different plasmids. V5-ER-GFP1-10 (ER targeted) and myc-mito-2XGFP11 (mitochondrial-targeted) (Cieri et al., 2018; Kakimoto et al., 2018). The two constructs were co-transfected in a 1:2 ratio, totaling 6 ug total DNA per MatTek dish. All mitophagy reporters were synthesized by Genscript.

Western Blot Analysis

Cells were collected by centrifugation at 600x g for 5 minutes and homogenized in ice-cold lysis buffer consisting of 50 mM Tris-HCl, 150 mM NaCl, 1 mM EGTA, 1 mM EDTA, 1% Triton X-100, and protease inhibitor mixture (Roche Applied Science, 11873580001). Lysates were cleared by centrifugation at 20,000 x g for 20 minutes at 4ºC, and protein concentrations were assessed by Bradford assay. Samples were prepared with Dithiothreitol (BioRad, 161-0611) and NuPAGE™ LDS Sample Buffer (4X) (Thermo Fisher NP0007) and boiled at 95ºC for 5 minutes. Samples were run on 10% or 12% NuPAGE Bis-Tris gels (Invitrogen, NP0302BOX) and transferred to nitrocellulose

membranes (GE Healthcare Life Sciences, 10600001). Membranes were stained with Ponceau S to observe total protein distribution, washed with Tris-buffered saline (TBS)-Tween, and then blocked with 5% milk in TBS-Tween for 1 hour. Membranes were incubated with the specified antibodies in 5% milk TBS-Tween overnight at 4º C, washed with TBS-Tween and incubated with species-specific anti-HRP secondary antibody in 5% milk TBS-Tween. Blots were developed with ECL dura solution (Thermo, 34076) and imaged with a Bio-Rad ChemiDoc XRS+ imager. Band densitometry quantification was performed using Image Lab 4.1 (Bio-Rad) software.

Primary Antibodies: Beclin1 (Santa Cruz, sc-11427), Actin (Genetex, 110003), GAPDH (GenTex, GTX627408), P62 (Abcam, ab56416), LC3 A/B (Cell Signaling, 4108), MTC01 (labeled as COXIV, Thermo, 459600), Parkin (Cell Signaling, 4211), Tim23 (BD Biosciences, 611222), Tom20 (Santa Cruz, 11415), Ubiquitin (Enzo, ABS840), Tubulin (Sigma, T6074), Myc (Sigma, M4439), Flag (Sigma, F7425). *Secondary Antibodies:* goat anti-mouse (Life Technologies, 31430), goat-anti-rabbit HRP (Life Technologies, 31460).

Immunofluorescent Staining

Cells were fixed using 4% formaldehyde solution (Thermo Fisher, 28906) in phosphate-buffered saline (PBS) and incubated at 37º C for 20 minutes. Cells were permeabilized using 0.2% Triton X-100 (Sigma, T9284) in PBS at 37º C for 30 minutes, followed by blocking in 5% normal goat serum (Vector labs, S-1000) for 45 minutes. Primary antibodies were used at 1:100 dilution in 5% normal goat serum and incubated at 4ºC overnight. After washes with PBS, cells were incubated with fluorescent secondary antibodies at 1:200 dilution.

Primary Antibodies: Beclin1 (Santa Cruz, sc-11427), MTC01 (labeled as COX IV, Thermo, 459600), Tim23 (BD Biosciences, 611222), Tom20 (Santa Cruz, 11415), Myc (Sigma, M4439), Flag (Sigma, F7425). Secondary Antibodies: Alexa Fluor 350 (Thermo Fisher, rb A11046, ms A11045), Alexa Fluor 488 (Thermo Fisher, rb A11034, ms A11029), Alexa Fluor 594 (Thermo Fisher, rb A11037, ms A11032) and Alexa Fluor 647 (Thermo Fisher, rb A21244, ms A21235).

Fluorescent Imaging

Fluorescence images were captured using a Nikon Eclipse Ti2-E with a motorized XYZ-stage fitted with a Plan-Apochromat lambda 60X NA 1.40 oil immersion objective. Z stacks were separated by 0.3 µM and acquired with a DS-Qi2 camera (Nikon) illuminated by a Solid-state White Light Excitation Source (Lumencor). Images were processed by 3D deconvolution and compressed into extended depth of focus (EDF) images by NIS-Elements AR GA3 software unless otherwise noted in figure legends. Image analysis was done using NIS elements software and Image J (Schneider et al., 2012).

Mitochondrial Isolation

Cells were collected and spun down at 2500 x g for 5 minutes at 4ºC, resuspended in 1 mL isolation buffer (220 mM mannitol, 70 mM sucrose, 1 mM EDTA, 10 mM HEPES) adjusted to pH7.4 with KOH and 1X protease inhibitor for 1 hour. Cells were manually homogenized using a plastic Eppendorf tube mortar and pestle for 10 minutes on ice to gently release mitochondria. The suspension was centrifuged at 1000 x g for 5 minutes at 4ºC to pellet cellular debris. The supernatant was spun at 14,000 x g at 4ºC for 15 minutes and the mitochondrial pellet was gently washed and resuspended in isolation buffer. Protein concentrations were assessed by Bradford assay.

Reverse Transcriptase Quantitative PCR

RNA was extracted from cells using the RNeasy Mini Kit (Qiagen, 74104) and quantified by Nanodrop (Thermo Fisher). Reverse transcription to cDNA was performed with the QuantiTect Reverse Transcription Kit (Qiagen, 205311) according to the manufacturer's protocol. qPCR was performed with standard TaqMan primers and TaqMan Universal Mastermix II (Applied Biosystems 4440040) or SYBR Green (Applied Biosystems, 4309155) on a CFX96 real-time PCR detection system (Bio-Rad Laboratories). Fold difference was calculated by the comparative C_T($2^{-\Delta\Delta C}$T) method against 18s ribosomal RNA (Schmittgen and Livak, 2008).

Primers for 18S *Rn18s* (18S Mm03928990), *Beclin1* primers were designed to recognize exon2 (FWD: 5'- GCATGGAGGGGTCTAAGGCGTC-3' and REV 5'- GTTCCTGGATGGTGACCCGGTC-3') and were obtained from Eton Bioscience Inc. *Beclin2* primers were (FWD: 5'- GCGCTCTCGAGGCTAGCATGTCTTCCATCC-3' and REV: 5'- GCGCTAAGCTTGGGCCCTCAAGCGTA-3') obtained from Integrated DNA Technologies.

Statistical Analysis

All experiments were performed independently and repeated a minimum of three times. Data are mean ± S.E.M. Differences between groups were assessed by repeated-measure ANOVA tests with Tukey or Dunnett's post hoc test using GraphPad Prism 6 software. Each test was used based on the number of samples being analyzed according to the test's assumptions and requirements. Differences were considered significant when $p < 0.05$. Analyses were done un-blinded with respect to sample identity. Scientific

justifications for data exclusion included very low transfection efficiency (<15%) or changes in cell viability under control conditions.

2.1 Acknowledgements

Parts of Chapter 2 are in preparation for a manuscript for submission to a journal. Gonzalez, E. R., Jeung, M., Gustafsson, Å. B. The primary author is the lead investigator and author of this manuscript.

CHAPTER 3: Beclin1 and Beclin2 in Autophagy

3.1 Introduction

Autophagy is an essential cellular degradation pathway that is enhanced by starvation and in response to stress (Dikic & Elazar, 2018; Guo et al., 2016). Beclin1 is a scaffolding protein that has been widely studied in the context of autophagy for its participation in the autophagosome initiation and maturation (Guo et al. 2016; Dikic and Elazar 2018). Its homolog, Beclin2 has also been implicated in autophagy but is less widely studied (He et al., 2013). Thus far, there have been no studies exploring the compensation mechanisms between Beclin1 and Beclin2, nor how autophagy is altered in cells lacking these proteins. In this chapter, we begin to explore these questions and, in the process, uncover a cell-type-specific stress response behavior of Beclin1. We also provide evidence of a Beclin1-and-Beclin2 independent autophagy pathway exists.

3.2 Results

Beclin1 has been reported to be an essential component of the autophagy PI3K complex that initiates formation of autophagosomes. Based on these findings, we first asked to what extent autophagy is altered in cells lacking Beclin1. Therefore, to measure Beclin1-dependent differences in autophagic flux, we treated wild type (WT) and *Becn1*$^{-/-}$ Mouse Embryonic Fibroblasts (MEFs) with Bafilomycin A1, a V-ATPase inhibitor that prevents autophagosome and lysosome fusion. Changes in levels to the lipidated form of Microtubule-associated protein 1A/1B-light chain 3 (LC3), known as LC3II, is commonly used to measure the formation of autophagosomes (Klionsky et al., 2021). Consistent with previous studies, we observed a significant accumulation of LC3II in WT MEFs after

3 hours of Bafilomycin A1 treatment (Klionsky et al., 2021). We also observed a significant increase in LC3II levels in *Becn1*$^{-/-}$ MEFs after Bafilomycin A treatment but reduced when compared to WT MEFs (Fig. 3.1A-B). In addition, we assessed levels of the autophagy adaptor p62, which accumulates in the presence of Bafilomycin A1 due to lack of degradation. We observed a similar increase in p62 levels in WT and *Becn1*$^{-/-}$ MEFs (Fig. 3.1A-B). Using GFP-LC3 to visualize autophagosomes, we found that the presence of Bafilomycin A1 led to the accumulation of GFP-LC3 positive autophagosomes in both WT and *Becn1*$^{-/-}$ MEFs (Fig. 3.1C-D). Overall, these findings suggest that Beclin1 deficient cells have reduced autophagosome formation but autophagic activity is still functional.

Autophagy is induced in response to various challenges, such as nutrient deprivation. To investigate if stress-induced autophagy is intact in the absence of Beclin1, we exposed WT and *Becn1*$^{-/-}$ MEFs to nutrient deprivation. Cells were incubated in DMEM +Glutamax, without Fetal Bovine Serum (FBS) for 3 hours. We observed similar levels of increase in LC3II after starvation in WT and *Becn1*$^{-/-}$ MEFs (Fig. 3.2A-B). Starvation also led to a similar formation of GFP-LC3 positive autophagosomes in both WT cells and cells lacking Beclin1 (Fig. 3.2C-D). We also assessed the dependency of autophagy on Beclin1 in response to a mitochondrial-specific stressor. We used the mitochondrial uncoupler trifluoromethoxy carbonyl cyanide phenylhydrazone (FCCP), which uncouples oxidative phosphorylation from membrane potential by increasing permeability to H+ (Demine et al., 2019). Consistent with previous findings, WT cells significantly increased amounts of LC3II protein following treatment with FCCP (Ashrafi & Schwarz, 2013). *Becn1*$^{-/-}$ MEFs, also generated a significant increase in LC3II levels, suggesting there is no inhibition to form autophagosomes in cells lacking Beclin1 when challenged by FCCP (Fig. 3.2E-H).

Together, these results indicate that the presence of Beclin1 is not essential for the formation of autophagosomes in response to stress in MEFs.

Very little is known about the function of Beclin2 in autophagy. Here, we investigated if Beclin2 levels were altered in the absence of Beclin1. Quantitative PCR (qPCR) showed that transcript levels of both *Becn1* and *Becn2* remain unchanged in WT MEFs in response to starvation or FCCP treatment (Fig. 3.3A). However, we observed a significant increase in *Becn2* transcript levels after exposure to stress but not at baseline (Fig. 3.3B). This indicates a potential compensation by Beclin2 may be needed whenever there is a greater demand for autophagy (Fig. 3.3B).

To further explore the function of Beclin2 in autophagy, we generated *BECN1*$^{-/-}$ and *BECN2*$^{-/-}$ HeLa cells by CRISPR-Cas9 multi-guide gene editing. We confirmed the successful knockout of *BECN1* by Western blot (Fig. 3.4A) and qPCR (Fig. 3.5A). While we were limited by a lack of commercially available Beclin2 antibodies, we confirmed the successful knockout of *BECN2* at the DNA and RNA levels by PCR (Fig. 3.4B) and qPCR (Fig. 3.5B). First, we examined whether Beclin1 levels changed in Beclin2-deficient cells or if Beclin2 levels changed in Beclin1-deficient cells. Similar to *Becn1*$^{-/-}$ MEFs, we only observed a significant increase in *BECN2* transcript levels after exposure to FCCP or starvation in *BECN1*$^{-/-}$ HeLa cells (Fig. 3.5A). Similarly, *BECN1* transcript levels were increased in *BECN2*$^{-/-}$ HeLa cells in response to stress (Fig. 3.5B). Together, these experiments indicate that knocking out either *BECN1* or *BECN2* in HeLa cells increases expression of the present homolog only in response to stress.

To characterize autophagic activity in the *BECN1*$^{-/-}$ and *BECN2*$^{-/-}$ HeLa cells, we first evaluated autophagic flux. After 4 hours of Bafilomycin A1 treatment, WT, *BECN1*$^{-/-}$

and *BECN2*$^{-/-}$ HeLa cells had significant increases in LC3II and p62 levels compared to control conditions. However, both *BECN1*$^{-/-}$ and *BECN2*$^{-/-}$ HeLa cells had reduced increases in LC3II levels compared to WT cells after Bafilomycin A1 treatment (Fig. 3.6A-B). Imaging experiments confirmed GFP-LC3 positive vesicles do form in the absence of Beclin1 or Beclin2 (Fig. 3.6C-D). These findings suggest that autophagosome formation is reduced in both *BECN1*$^{-/-}$ *and BECN2*$^{-/-}$ HeLa cells.

Next, we challenged WT, *BECN1*$^{-/-}$ *and BECN2*$^{-/-}$ HeLa cells with autophagy-inducing stressors. Serum starvation did not generate a significant difference between WT, *BECN1*$^{-/-}$ and *BECN2*$^{-/-}$ HeLa LC3II levels or total number of GFP-LC3 vesicles formed (Fig. 3.7A-D). In contrast, following mitochondrial-specific stressor FCCP treatment, *BECN1*$^{-/-}$ and *BECN2*$^{-/-}$ HeLa cells had significantly reduced LC3II levels compared to WT cells (Fig. 3.7E-F). However, observations of vesicles formed by imaging GFP-LC3 revealed autophagosome formation was intact (Fig. 3.7G-H). Overall, these experiments show that although both Beclin1 and Beclin2 deficient cells can form autophagosomes, the formation of autophagosomes is reduced in response to specific stressors.

Thus far, our findings suggest that neither Beclin1 nor Beclin2 alone are essential for autophagosome formation. Therefore, we decided to use a siRNA to knockdown Beclin1 in the *BECN2*$^{-/-}$ HeLa cells. After 72 hours of transfection with siRNA against Beclin1, we treated cells with BafilomycinA1 to assess autophagic flux. Intriguingly, we observed that these cells were still capable of forming autophagosomes at baseline, although at a reduced level (Fig. 3.8A-B). This also suggests that both Beclin1 and Beclin2 contribute to autophagosome formation at baseline but that an alternative

pathway also exists. In contrast, both starvation and FCCP treatments promoted a significant increase in LC3II levels in cells lacking Beclin1 and Beclin2, and we observed no comparative difference to control *BECN2*$^{-/-}$ HeLa cells (Fig. 3.8C-F). These results suggest a Beclin1-and-Beclin2-independent autophagy pathway can be activated in response to stress in cells lacking both Beclin1 and Beclin2.

3.3 Discussion

The present study demonstrates that neither Beclin1 nor Beclin2 are essential to autophagosome formation. Future studies should focus on identifying the Beclin1 and Beclin2 independent autophagy pathways that clearly exist in cells.

Both mouse and human cell lines displayed intact, albeit reduced, autophagosome formation at baseline in the absence of Beclin1 and Beclin2. These findings indicate that both Beclin1 and Beclin2 contribute to, but are not essential for, autophagic flux.

Responses to autophagy-inducing stressors revealed potential cell-type-specific functions of Beclin1. Mouse cell lines lacking Beclin1 were able to form autophagosomes in response to both starvation and FCCP treatment at rates comparable to WT cells. This suggests that murine Beclin1 is not required for the activation of autophagy in response to general stressors or specific autophagy-inducing stimuli. However, human cell lines lacking Beclin1 exhibited reduced ability to form autophagosomes only in response to FCCP. These differences suggest Beclin1 may have variable responsibilities in species (mouse vs human) or cell type.

Based on our observations by qPCR, we observed that Beclin1 and Beclin2 transcripts were upregulated in the absence of the other, but only in response to stress.

Analysis of mouse cells lacking Beclin1, show upregulation of *Becn2* transcript levels during stress. These cells maintain autophagosome formation, which could indicate a Beclin2 compensatory mechanism is sufficient in mouse cells. However, in human cells lacking Beclin1, where autophagosome formation is not restored in response to stress, the compensatory upregulation of Beclin2 may not be sufficient. Therefore, in addition to potential species or cell-type-specific roles for Beclin1, there may also be cell-type-specific compensatory mechanisms to maintain this essential homeostatic process. However, the precise dependency on compensatory mechanisms between species requires further investigation.

Additionally, we observe cells lacking both Beclin1 and Beclin2 still have functional autophagy, which strongly suggests activation of a Beclin1-and-Beclin2- independent autophagy pathway. This prompts the questions: when, how, and which Beclin1-and-Beclin2 independent autophagy pathways get activated? The Beclin1 and Beclin2 deficient cell lines generated in these studies may be useful for dissecting these processes in future investigations.

3.4 Acknowledgments

Parts of Chapter 3 are in preparation for a manuscript for submission to a journal. Gonzalez, E. R., Jeung, M., Gustafsson, Å. B. The primary author is the lead investigator and author of this manuscript.

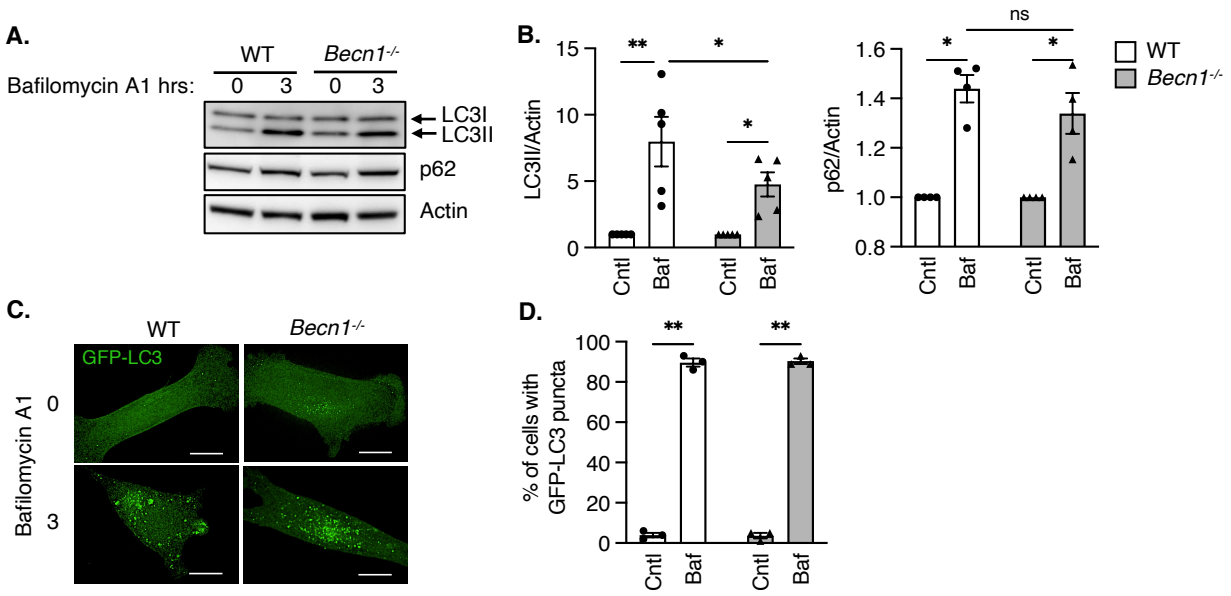

Figure 3.1 Beclin1-deficient MEFs have reduced autophagosome formation. A) Representative Western blot of LC3 and p62 levels in WT and *Becn1*$^{-/-}$ MEFs at baseline and after Bafilomycin A1 treatment (100nm, 3 hrs). B) Quantification of LC3II and p62 protein levels A (n=4-5; *p<0.05, **p<0.01, ns = not significant). C) Representative immunofluorescent images of MEFs overexpressing GFP-LC3 before (0h) or after Bafilomycin A1 treatment (100nm, 3h) (scale bars = 10 μm). D) Quantification of the total percent of cells with GFP-LC3 positive vesicles (n=3, 100 cells/experiment, **p<0.01). Statistical test: One-way analysis of variance (ANOVA) followed by Tukey's multiple comparison test.

Figure 3.2 Beclin1-deficient MEFs have intact autophagic activity. A) Representative Western blot of LC3 levels in WT and *Becn1*$^{-/-}$ MEFs after starvation in DMEM+ Glutamax with no FBS for 3hr. B) Quantification of LC3II protein levels (n=5, *p<0.05, ns=not significant). C) Representative immunofluorescent images of overexpressed GFP-LC3 in WT and *Becn1*$^{-/-}$ MEFs before (0) or after 3 hours (3) starvation (scale bars = 10 μm). D) Quantification of the total percentage of cells with GFP-LC3 positive vesicles from C (n=3, 100 cells/experiment, **p<0.01). E) Representative Western blot of LC3 levels in WT and *Becn1*$^{-/-}$ MEFs after 25 μM FCCP treatment for 3 hrs. F) Quantification of LC3II protein levels (n=5, *p<0.05, **p<0.01, ns = not significant). G) Representative immunofluorescent images of GFP-LC3 in WT and *Becn1*$^{-/-}$ MEFs after FCCP treatment (25 μM, 3h) (scale bars = 10 μm). H) Quantification of the total percentage of cells with GFP-LC3 positive vesicles (n=3, 100 cells/experiment, **p<0.01). Statistical test: Two-way analysis of variance (ANOVA) followed by Tukey's multiple comparison test.

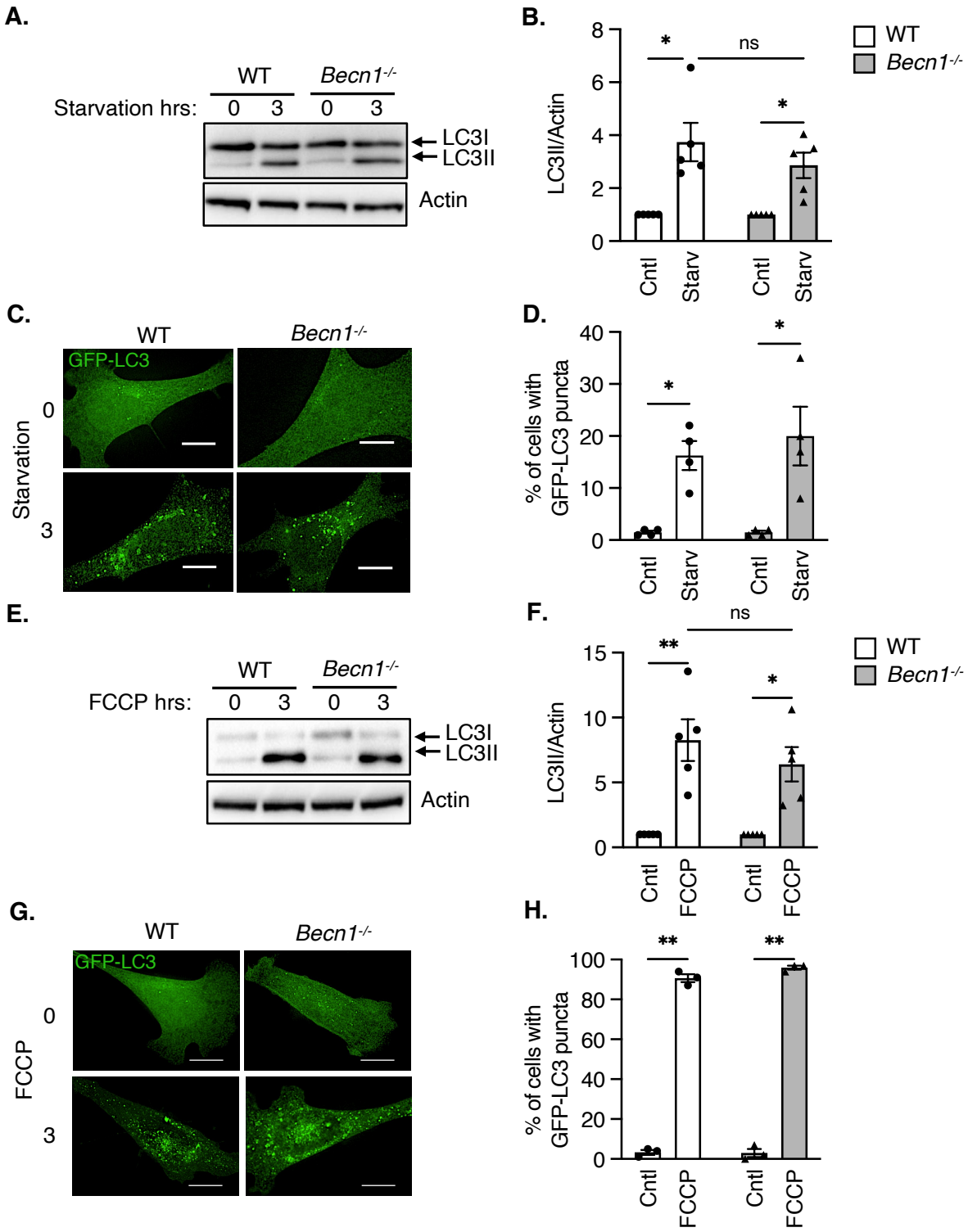
A.
WT
Becn1-/-
Starvation hrs:
0
3
0
3
LC3I
LC3II
Actin
B.
LC3II/Actin
ns
WT
Becn1-/-
Cntl
Starv
Cntl
Starv
C.
WT
Becn1-/-
GFP-LC3
Starvation
0
3
D.
% of cells with GFP-LC3 puncta
E.
FCCP hrs:
F.
FCCP
G.
H.

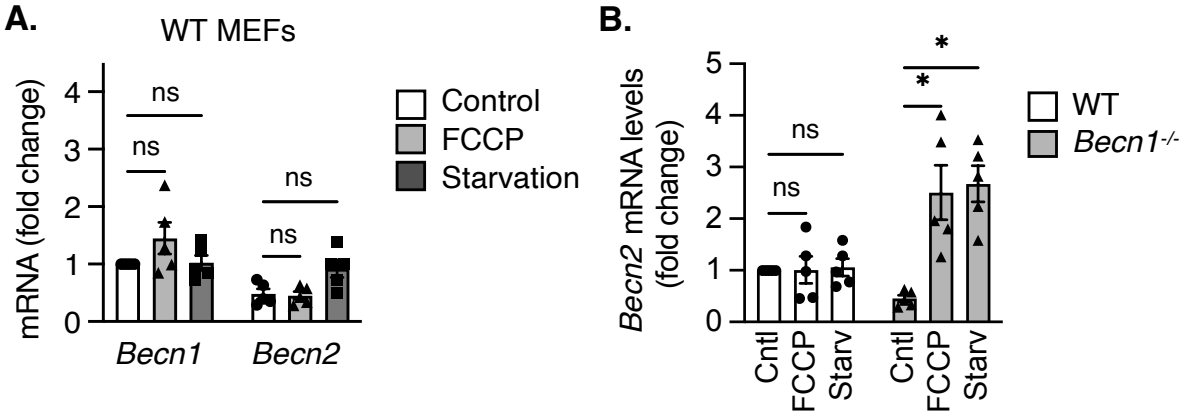

Figure 3.3 Beclin1-deficient MEFs upregulate *Becn2* in response to autophagy inducing stress. A) qPCR with reverse transcription analysis of *Becn1* and *Becn2* transcript levels in WT MEFs at baseline (control) and in response to FCCP (25 μM, 3 hrs) or starvation (DMEM+ Glutamax with no FBS, 3hrs) (n=5, ns = not significant). B) qPCR analysis of *Becn2* transcripts in WT and *Becn1*$^{-/-}$ MEFs at baseline (cntl) and in response to FCCP and starvation (n=5, *p<0.05, ns = not significant). Statistical test: One-way analysis of variance (ANOVA) followed by Tukey's multiple comparison test.

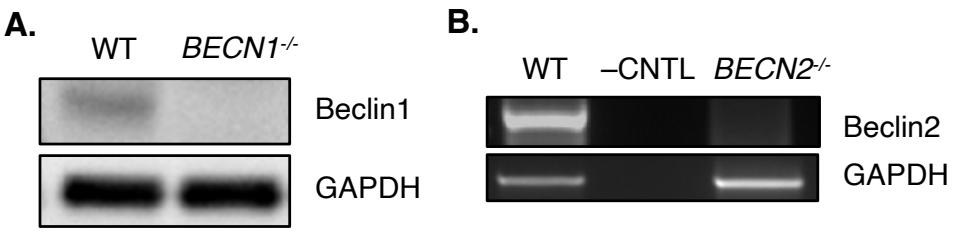

Figure 3.4 Confirmation of HeLa knockout cell lines generated by CRISPR-Cas9 Gene Editing. A) Representative Western blot of Beclin1 protein levels in WT and *BECN1*$^{-/-}$ HeLa cells. B) Ethidium Bromide Gel of PCR- amplified *BECN2* transcript levels in WT and *BECN2*$^{-/-}$ HeLa cells (-CNTL; no template DNA).

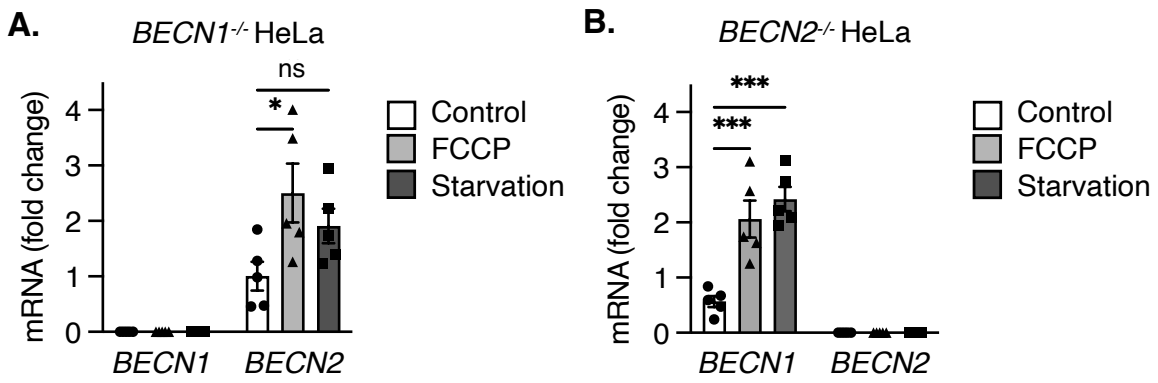

Figure 3.5 *BECN1* and *BECN2* transcript levels increase in *BECN1*$^{-/-}$ or *BECN2*$^{-/-}$ HeLa cells after stress. A) Quantitative PCR of *BECN1* and *BECN2* transcript levels in *BECN1*$^{-/-}$ HeLa cells (n=5, *p<0.05, ns = not significant) D) Quantitative PCR analysis of *BECN1* and *BECN2* transcript levels in *BECN2*$^{-/-}$ HeLa cells (n=5, ***p<0.001).

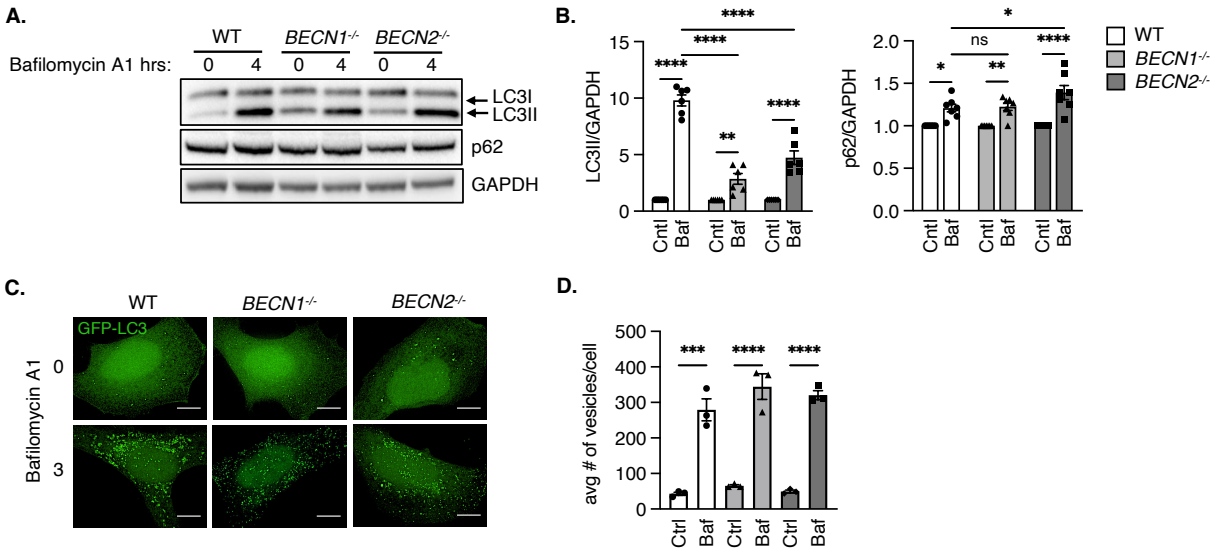

Figure 3.6 Beclin1 and Beclin2-deficient HeLa cells have reduced baseline autophagosome formation. A) Representative Western blot of LC3 levels in WT, *BECN1*$^{-/-}$ and *BECN2*$^{-/-}$ HeLa cells after 100 nM Bafilomycin A1 treatment for 4 hrs. B) Quantification of LC3II protein levels (n=6, **p<0.01, ***p<0.001, ****p<0.0001, ns = not significant). C) Representative immunofluorescent images of GFP-LC3 in WT, *BECN1*$^{-/-}$ and *BECN2*$^{-/-}$ HeLa cells before (0h) and after Bafilomycin A1 treatment (100nm, 3h) (scale bars = 10 μm). D) Quantification of the number of GFP-LC3 positive vesicles per cell (n=3, 100 cells/experiment, *p<0.05, ns = not significant) (scale bars = 10 μm). Statistical test: Two-way analysis of variance (ANOVA) followed by Tukey's multiple comparison test.

Figure 3.7 Beclin1 and Beclin2-deficient HeLa cells have reduced autophagosome formation in response to stress. A) Representative Western blot of LC3 levels in WT, *BECN1*$^{-/-}$, and *BECN2*$^{-/-}$ HeLa cells after starvation in DMEM+ Glutamax without FBS for 3hrs. B) Quantification of LC3II protein levels (n=5, **p<0.01, ns = not significant). C) Representative immunofluorescent images of overexpressed GFP-LC3 in WT, *BECN1*$^{-/-}$, and *BECN2*$^{-/-}$ HeLa cells before (0) and after (3) starvation (scale bars = 10 μm). D) Quantification of the number of GFP-LC3 positive vesicles per cell (n=3, 100 cells/experiment, *p<0.05, **p<0.01). E) Representative Western blot of LC3 levels in WT, *BECN1* and *BECN2*$^{-/-}$ HeLa cells after 25 μM FCCP for 3 hrs. F) Quantification of LC3II protein levels (n=5, *p<0.05, **p<0.01, ***p<0.001). G) Representative immunofluorescent images of GFP-LC3 in WT, *BECN1*$^{-/-}$ and *BECN2*$^{-/-}$ HeLa cells before (0) and after 3 hours (3) of 10 μM FCCP treatment (scale bars = 10 um). H) Quantification of the number of GFP-LC3 positive vesicles per cell (n=3, 100 cells/experiment, **p<0.01). Statistical test: Two-way analysis of variance (ANOVA) followed by Tukey's multiple comparison test.

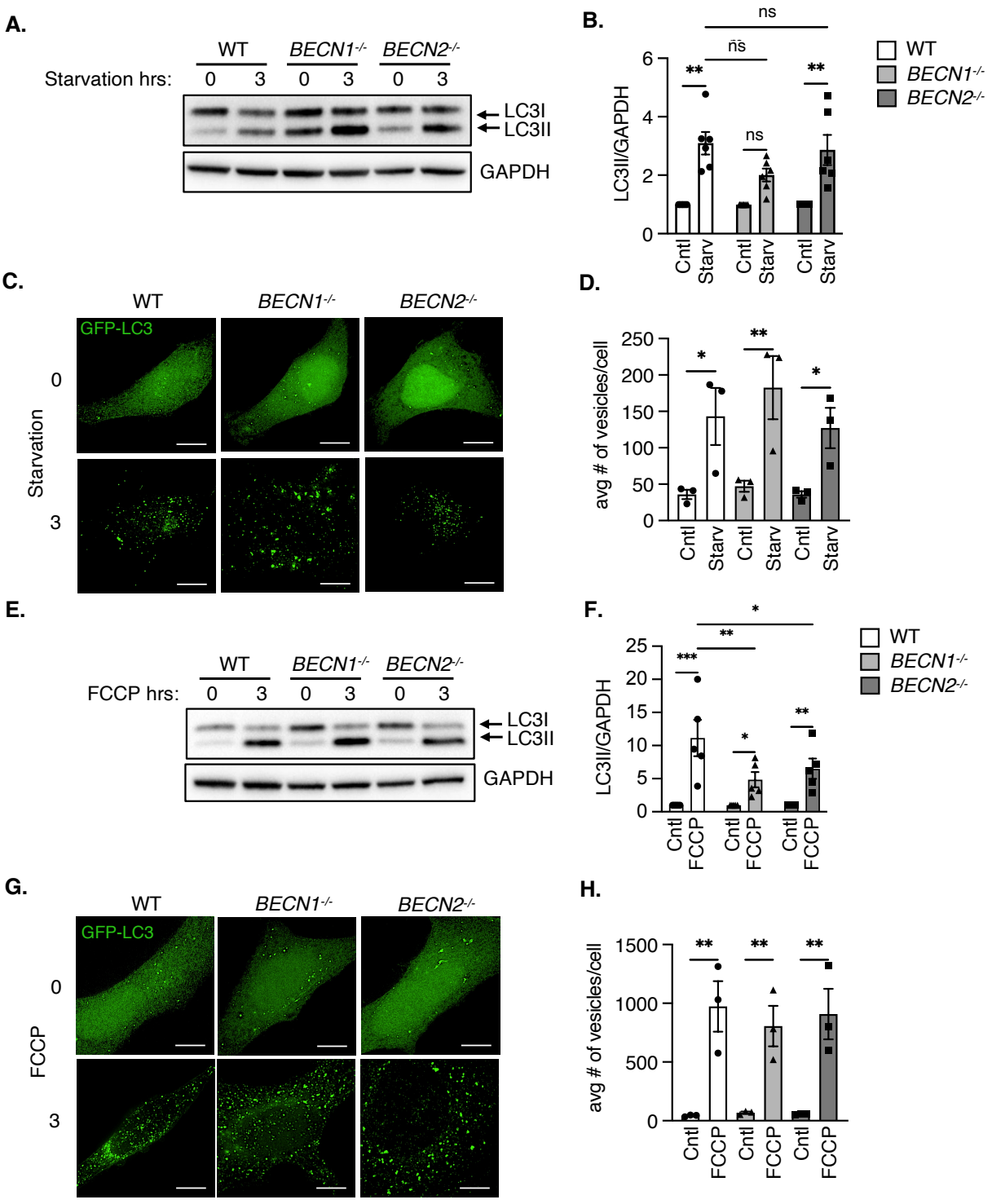
A.
WT
BECN1-/-
BECN2-/-
Starvation hrs:
0 3 0 3 0 3
LC3I
LC3II
GAPDH
B.
ns
ns
**
ns
**
LC3II/GAPDH
6
4
2
0
Cntl
Starv
WT
BECN1-/-
BECN2-/-
C.
WT
BECN1-/-
BECN2-/-
GFP-LC3
Starvation
0
3
D.
avg # of vesicles/cell
250
200
150
100
50
0
*
**
*
Cntl
Starv
E.
WT
BECN1-/-
BECN2-/-
FCCP hrs:
0 3 0 3 0 3
LC3I
LC3II
GAPDH
F.
*
**
***
*
**
LC3II/GAPDH
25
20
15
10
5
0
Cntl
FCCP
WT
BECN1-/-
BECN2-/-
G.
WT
BECN1-/-
BECN2-/-
GFP-LC3
FCCP
0
3
H.
avg # of vesicles/cell
1500
1000
500
0
**
**
**
Cntl
FCCP

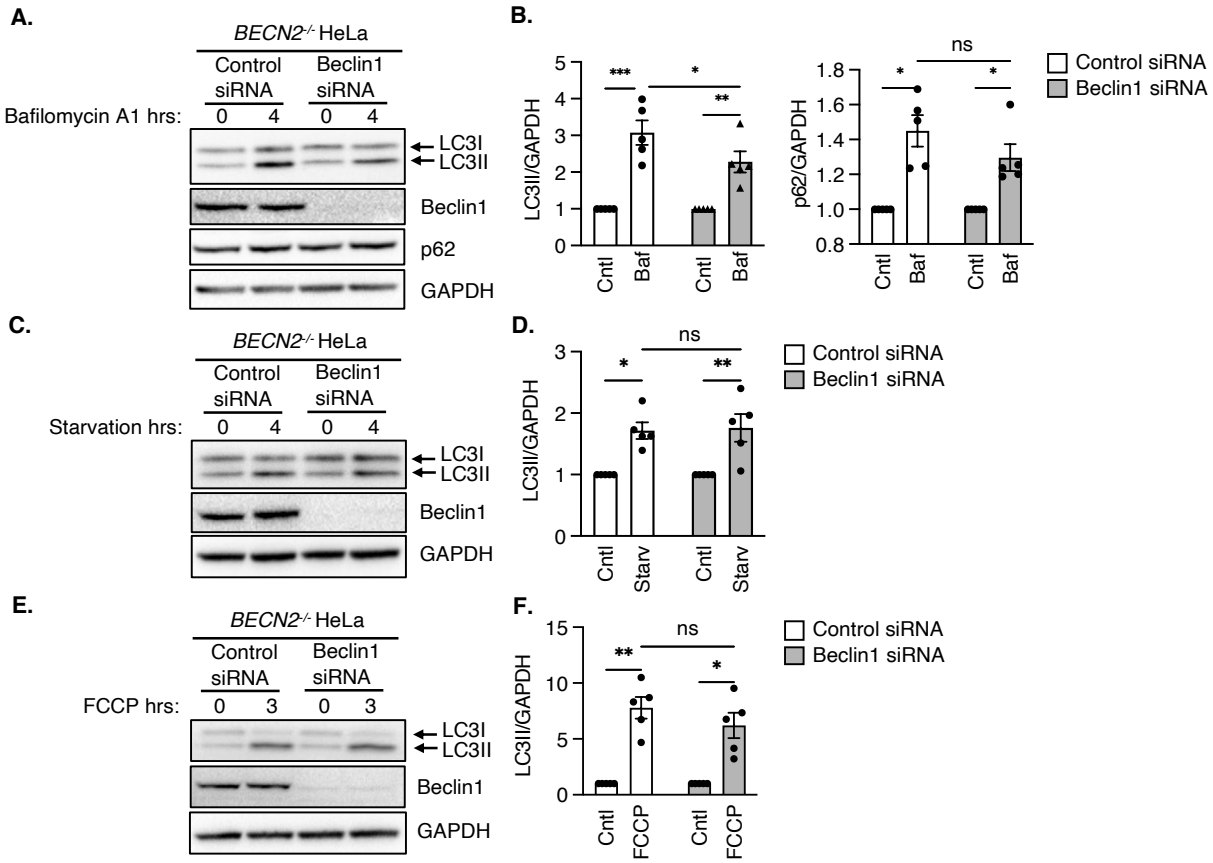

Figure 3.8 Knockdown of Beclin1 and Beclin2 in HeLa cells has no effect on autophagosome formation in response to stress. A) Representative Western blot of LC3, Beclin1 and p62 levels in *BECN2*$^{-/-}$ HeLa cells transfected with either control siRNA or Beclin1 siRNA and treated with 100nM Bafilomycin A1 for 4 hrs. B) Quantification of LC3II and p62 protein levels (n=5, **p<0.01, ***p<0.001, ns = not significant). C) Representative Western blot of LC3 and Beclin1 levels in *BECN2*$^{-/-}$ HeLa cells transfected with either control siRNA or Beclin1 siRNA after incubation in DMEM+ Glutamax with no FBS for 4 hrs. D) Quantification of LC3II protein levels (n=5, *p<0.05, **p<0.01, ns = not significant). E) Representative Western blot of LC3 and Beclin1 levels in *BECN2*$^{-/-}$ HeLa cells transfected with either control siRNA or Beclin1 siRNA and treated with 25 μM FCCP for 3 hrs. F) Quantification of LC3II protein levels (n=5, *p<0.05, **p<0.01, ns = not significant). Statistical test: Two-way analysis of variance (ANOVA) followed by Tukey's multiple comparison test.

CHAPTER 4: Beclin1 and Beclin2 in Mitophagy

4.1 Introduction

Mitophagy is a key process that contributes to mitochondrial homeostasis by selectively removing damaged organelles from the cell. Beclin1 has previously been implicated in mitophagy via interaction with PINK1, but the exact mechanisms are still unclear (Pickles et al., 2018). Beclin2 has not been convincingly implicated in mitophagy, therefore investigation of its potential involvement is needed. In this chapter, we dissect how Beclin1 functions in Parkin-mediated mitophagy. Additionally, we establish that Beclin2 is not involved in mitophagy by multiple approaches. Overall, this chapter contributes to the understanding of Beclin1's role in mitochondrial clearance.

4.2 Results

First, we generated a modified mitophagy reporter to assess mitophagy events via fluorescent imaging. This reporter consists of a mitochondrial targeting sequence (MTS) on the N-terminus, followed by a mCherry fluorescent tag, a pHluorin2 fluorescent tag, and a mitochondrial transmembrane (TM) domain that anchors this reporter to face the inner mitochondrial matrix. In a healthy mitochondrion, both the mCherry and pHluorin2 fluoresce, appearing as a yellow mitochondrion when the two imaged channels are overlaid (Fig. 4.1A). Unhealthy or damaged mitochondria undergoing mitophagy are engulfed by autophagosomes. Once autophagosomes merge with lysosomes, the lower pH environment inside the autophagolysosome quenches the pHluorin2 fluorescence. The mCherry is stable at lower pH and the mitochondria inside the autophagolysosome

then appear as red only (Fig. 4.1A)(Mahon, 2011). The generation of this new mitophagy reporter is explained in detail in Chapter 5 of this thesis.

We overexpressed the mitophagy reporter and Myc-Parkin to evaluate Parkin-mediated mitophagic clearance in response to a mitochondria-specific stressor. Mitochondrial-specific stress was induced with Oligomycin, an ATP synthase inhibitor, and Antimycin A, a complex III inhibitor (OA). This combination is often used to induce mitophagy in cells (Pickrell & Youle, 2015). In WT and *BECN2*$^{-/-}$ HeLa cells, we observed a significant increase in the number of mitophagy events following 12 hours of OA treatment. We did not see a similar increase in *BECN1*$^{-/-}$ HeLa cells (Fig. 4.1B-C). We confirmed these observations with Western blot analysis of the mitochondrial protein COX IV, in response to OA treatment and FCCP (Fig 4.2A-D). These experiments demonstrate that Beclin1 plays a role in Parkin-mediated mitophagy in HeLa cells.

We also confirmed a role for Beclin1 in mitophagy in MEFs. We observed that Beclin1-deficient MEFs have impaired mitochondrial clearance in response to FCCP treatment as assessed by western blotting for COX IV (Fig 4.3A-B). Imaging experiments using the mitophagy reporter confirmed that FCCP treatment led to a significant increase in mitophagy events in WT, but not in *Becn1*$^{-/-}$ MEFs (Fig 4.3 C-D). Together, these results indicate Beclin1 has a function in Parkin-mediated mitophagy in both MEFs and HeLa cells.

Based on our observations of reduced mitophagy, we wanted to investigate if there was an accumulation of dysfunctional mitochondria in the *Becn1*$^{-/-}$ MEFs. Mitochondrial morphology is often altered when aberrant mitochondria are present. However, we used fluorescent imaging to verify that there were no differences in mitochondrial morphology

in WT and *Becn1*$^{-/-}$ MEFs (Fig. 4.4A). Additionally, analysis of mitochondrial respiration by Seahorse assay showed no difference in oxidative capacity between WT and cells lacking Beclin1 (Fig. 4.4B). This suggests that Beclin1 has no effect on mitochondrial function.

Next, we dissected how Beclin1 functions in the mitophagy pathway. We examined the following intermediate steps: 1) Parkin translocation 2) Ubiquitination of the outer membrane 3) autophagosome localization to Parkin labeled mitochondria (Fig 1.3) (Pickles et al., 2018). We first examined Parkin recruitment to damaged mitochondria following FCCP treatment. Both WT and *Becn1*$^{-/-}$ MEFs had clear translocation of Parkin to damaged mitochondria after FCCP exposure (Fig. 4.5A-B). Additionally, we confirmed that Parkin translocation was associated with increased ubiquitination of mitochondrial proteins following FCCP exposure (Fig. 4.5C-D).

Next, we evaluated the colocalization of autophagosomes with Parkin-labeled mitochondria. In WT MEFs, we observed significant colocalization between GFP-LC3 positive autophagosomes and mCherry-Parkin after stress. In contrast, we observed significantly fewer colocalization events after stress in *Becn1*$^{-/-}$ MEFs (Fig. 4.6A-B). This suggests that Beclin1 is involved in the targeting of autophagosomes to dysfunctional mitochondria that have been labeled for mitophagy. Overexpression of Beclin1 in *Becn1*$^{-/-}$ MEFs restored the engulfment of mitochondria by autophagosomes, whereas overexpression of Beclin2 did not (Fig. 4.6A-B). These findings suggest that only Beclin1, and not Beclin2, has a specific function in mitophagy.

To further investigate the regulation of autophagosome targeting by Beclin1, we examined several phosphorylation sites on Beclin1 that may regulate its participation in

mitophagy (Menon & Dhamija, 2018, p. 1). The kinases involved in targeting these residues are commonly involved in mitophagy and thus merited further investigation. We generated phospho-mutant constructs of Beclin1 by changing selective residues for alanine's: Ser15, Ser30, Thr57, Ser90, and Ser93 (Fig. 4.7A). These constructs were overexpressed in Beclin1-deficient MEFs to determine to what extent each mutant was able to rescue the mitophagic defects in these cells. Evaluation of colocalization between GFP-LC3 labeled autophagosomes and mCherry-Parkin positive mitochondria revealed that cells expressing phospho-mutants Ser30, Thr57, Ser90, and Ser93 restored colocalization to WT levels (Fig. 4.7B-C). Only Beclin1S15A was unable to restore LC3 and Parkin colocalization levels (Fig. 4.7B-C). These results indicated that the Ser15 residue contributes to the proper targeting of autophagosomes to damaged mitochondria.

The final output of the mitophagy process is the degradation of damaged mitochondria. Thus, to further evaluate mitophagy restoration by the phospho-mutants, we overexpressed the mitophagy reporter and myc-Parkin in *Becn1*$^{-/-}$ MEFs. Following FCCP treatment, we observed restoration of mitophagy by all mutants except Beclin1S15A. Cells overexpressing Beclin1 had comparable mitophagy events when compared to WT (Fig. 4.8A-B). This implies that the phosphorylation of the Ser15 residue on Beclin1 contributes to the clearance of damaged mitochondria.

The Ser15 residue on Beclin1 is phosphorylated by Ulk1 (Russell et al., 2013). To further understand the role of Ulk1 in mitophagy, we treated cells with a Ulk1 inhibitor (SBI-0206965) with and without FCCP (Lin & Hurley, 2016). We found that WT MEFs treated with the Ulk1 inhibitor had reduced mitochondrial clearance compared to controls, as indicated by loss of the mitochondrial protein COX IV (Fig. 4.9A-B). This led us to

evaluate how the elimination of Ulk1 might influence Parkin-mediated mitophagy. As previously established, *Ulk1*$^{-/-}$ MEFs showed impaired mitochondrial clearance compared with WT cells following FCCP treatment (Tian et al., 2015). Imaging experiments revealed that similar to *Becn1*$^{-/-}$ MEFs, *Ulk1*$^{-/-}$ MEFs have reduced targeting of GFP-LC3 positive autophagosomes to Parkin-labeled mitochondria (Fig. 4.9C). Together, these experiments confirm the importance of Ulk1 and Beclin1 in regulating mitophagy.

It has been previously established that autophagosomes form at mitochondria-ER associated membranes (MAMs) (Hamasaki et al., 2013; Rubinsztein et al., 2012). Also a study has found that Beclin1 associates with MAMs (Gelmetti et al., 2017). Therefore, we sought to understand the connection between Beclin1 and Ulk1 at these contact sites. To observe MAMs in cells, we generated a split-GFP reporter with high similarity to previously created versions (Calì et al., 2019; Cieri et al., 2018). GFP1-10 is anchored in the ER, while GFP11 is anchored to the mitochondrion; individually, these two proteins do not fluoresce. When the two fragments of GFP are within 10 nm of each other, however, they fuse to form a full GFP protein and emit a signal when excited (Fig. 4.10A) (Calì et al., 2019; Cieri et al., 2018). This reporter allows for a highly sensitive visualization of mitochondrion-ER interface sites in cells.

We first confirmed the association of Beclin1 with MAMs by imaging. In agreement with previous reports, we observed Beclin1 puncta often resides near MAM structures at baseline (Gelmetti et al., 2017). Additionally, we observed an increase in the total number of MAMs after treatment with FCCP, which was accompanied by an increased association of Beclin1 puncta with MAMs (Fig. 4.10B). This data suggests that Beclin1 increases its interaction with MAMs in response to stress.

We next asked if MAM formation was affected in cells lacking Beclin1. Interestingly, we observed a significant difference between the number of MAMs in WT MEFs compared to Beclin1-deficient MEFs at baseline. However, the number of MAMs was significantly increased in both WT and *Becn1*$^{-/-}$ MEFs after treatment with FCCP (Fig. 4.10C-D). This suggests that although Beclin1 might contribute to the formation of MAMs at baseline, stress-induced increases in MAMs occur independently of Beclin1.

4.3 Discussion

In this chapter, I report on Beclin1's specific involvement in mitophagy. First, we determined that both mouse and human cells lacking Beclin1 have impaired Parkin-mediated clearance of mitochondria. Upon further investigation, we confirmed reduced clearance was due to impaired targeting of autophagosomes to dysfunctional mitochondria that had been labeled for mitophagy.

Interestingly, we observed that Beclin2 is not required for mitophagy. Instead, delivery of mitochondria to lysosomes is enhanced in Beclin2-deficient cells compared to WT cells, despite reduced formation of autophagosomes. The mechanism by which Beclin2-deficient cells have increased mitochondrial clearance compared to mitophagy will need to be investigated in future studies.

We used different phosphorylation-resistant mutants to first investigate the regulatory mechanisms that promote Beclin1's role in mitophagy. Next, we connected Ulk1-mediated phosphorylation of Serine 15 in Beclin1 to the targeting of autophagosomes to damaged mitochondria. Phosphorylation of Beclin1 by Ulk1 at Serine 15 and Serine 30 had previously been established and linked to kinase activation and

autophagosome initiation (Park et al., 2018; Russell et al., 2013). Here, we further revealed that Ulk1's phosphorylation of Beclin1 at Serine15 also functions in autophagosome targeting.

Moreover, we confirmed Beclin1 association with MAMs increases after the induction of mitophagy. We expanded on this by demonstrating that *Becn1*$^{-/-}$ MEFs have a reduced number of MAMs at baseline but can still increase the total number of membrane contacts after stress. While the overall number of MAMs in *Becn1*$^{-/-}$ MEFs under stress conditions remains lower than those in WT MEFs. This increase suggests a Beclin1-independent mechanism is involved in stress-induced mitophagy. Collectively, these data suggest that lower MAMs at baseline conditions predispose *Becn1*$^{-/-}$ MEFs to have less overall autophagosome targeting and mitophagic clearance.

4.4 Acknowledgements

Parts of Chapter 4 are in preparation for a manuscript for submission to a journal. Gonzalez, E. R., Jeung, M., Gustafsson, Å. B. The primary author is the lead investigator and author of this manuscript.

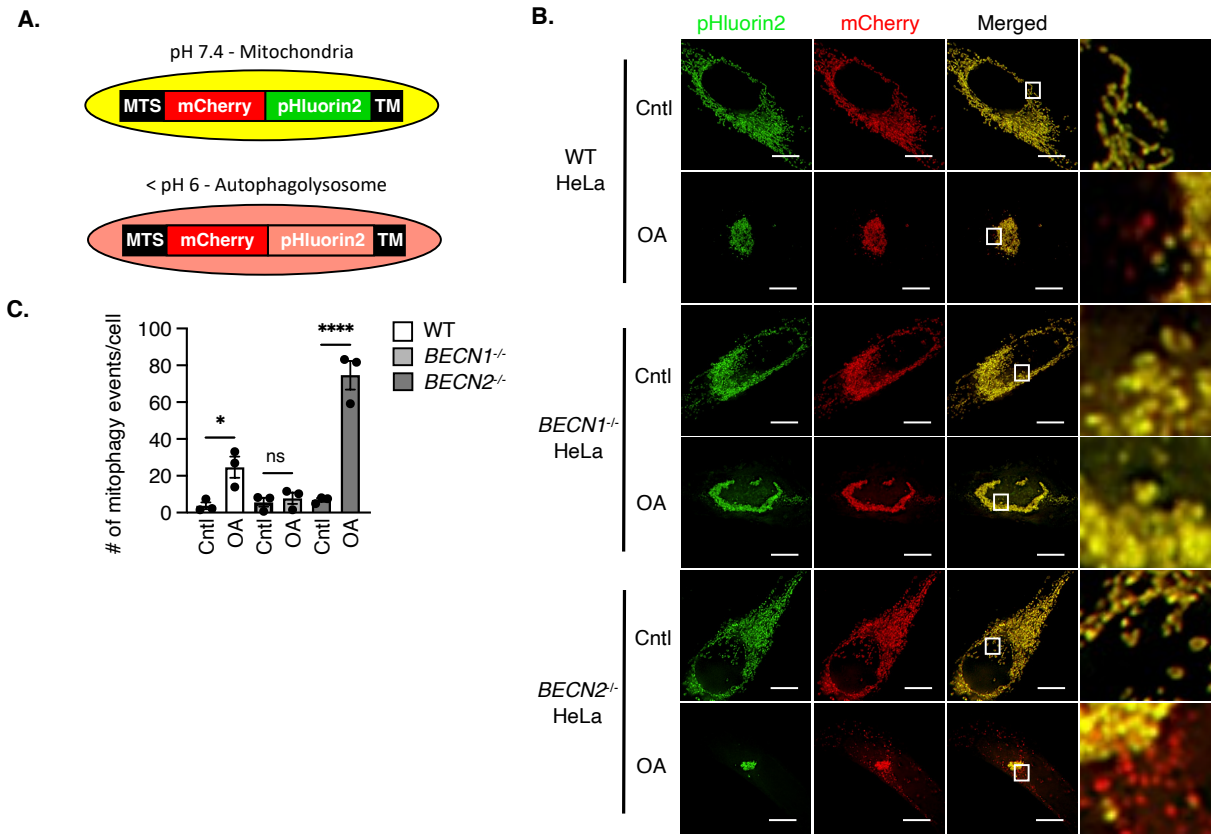

Figure 4.1 Beclin1-deficient HeLa cells have fewer mitophagy events. A) Schematic of mitophagy reporter design and fluorescent behavior at normal vs low pH. B) Representative images of *BECN1*$^{-/-}$ and *BECN2*$^{-/-}$ HeLa cells overexpressing the mitophagy reporter and myc-Parkin (not shown), challenged with Oligomycin (10 μM) and Antimycin A (4 μM)(OA) for 12 hrs (scale bar = 10 μm). C) Quantification of mitophagy events as measured by the number of red-only puncta after subtraction of yellow signal (n=3, 30 cells/experiment imaged, ns = *p<0.05, ****p<0.0001, ns = not significant) (scale bars = 10 μm). Statistical test: Two-way analysis of variance (ANOVA) followed by Tukey's multiple comparison test.

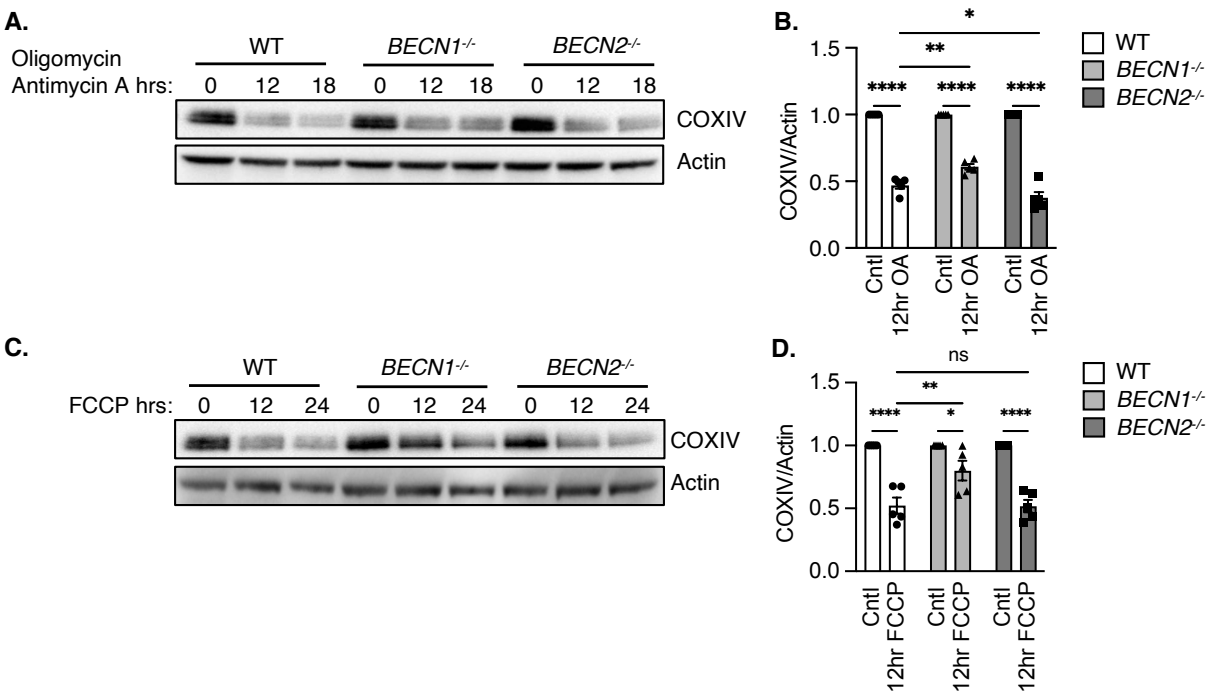

Figure 4.2 Beclin1-deficient HeLa cells have impaired Parkin-mediated mitochondrial clearance. A) Representative Western blot of COX IV levels in WT, *BECN1*$^{-/-}$ and *BECN2*$^{-/-}$ HeLa cells treated with Oligomycin (10 μM) plus Antimycin A (4 μM) (OA) for 12 hrs or 18 hrs. B) Quantification of COX IV protein levels at 12 hrs (n=5, **p<0.01, ***p<0.001, ****p<0.0001). C) Representative Western blot of COX IV levels in WT, *BECN1*$^{-/-}$ and *BECN2*$^{-/-}$ HeLa cells treated with 25 μM FCCP for 12 hrs or 24 hrs. D) Quantification of COX IV protein levels at 12 hrs (n=5, *p<0.05, **p<0.01, ****p<0.0001). Statistical test: Two-way analysis of variance (ANOVA) followed by Tukey's multiple comparison test.

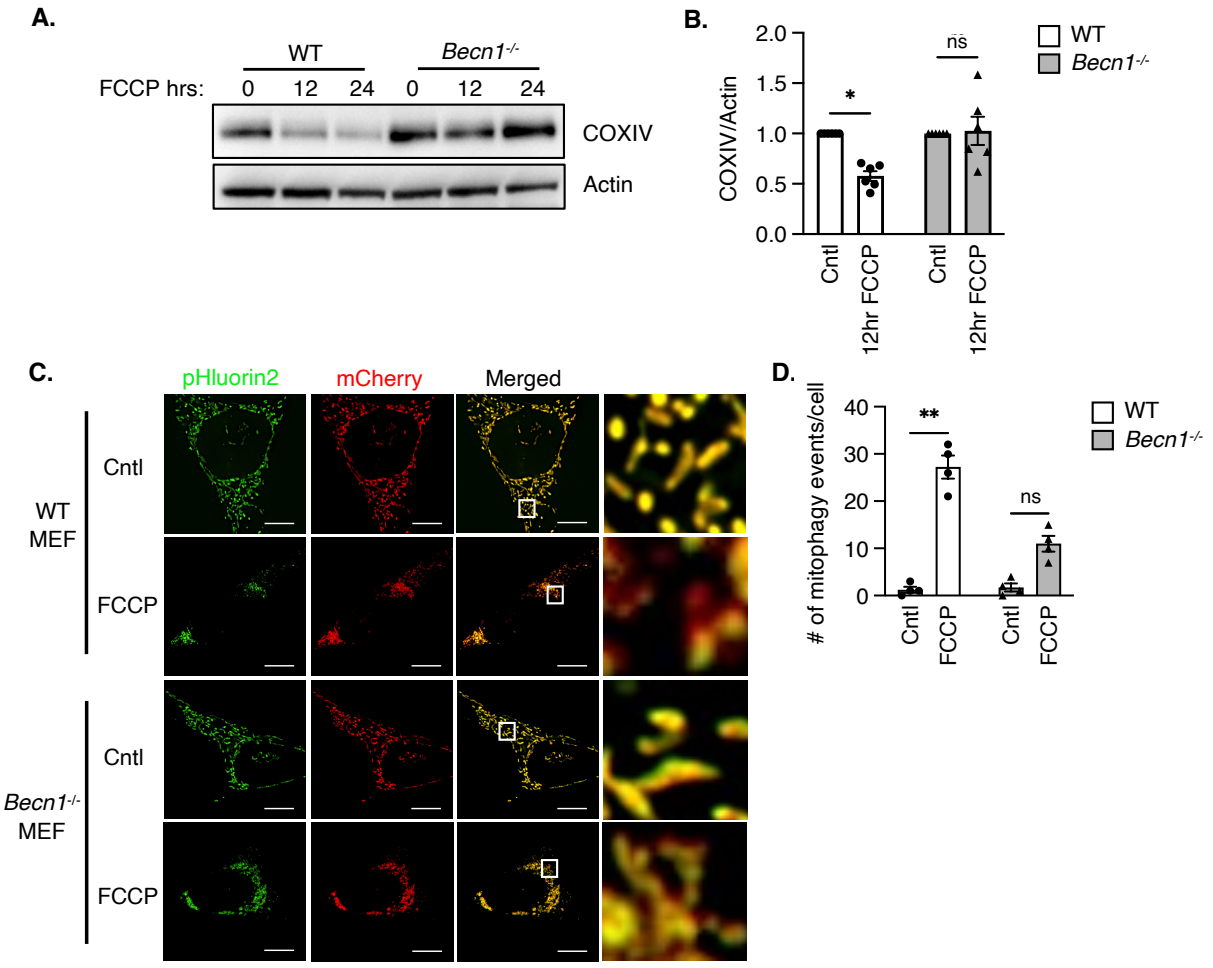

Figure 4.3 Beclin1-deficient MEFs have impaired Parkin-mediated mitochondrial clearance. A) Representative Western blot of COX IV levels in WT and *Becn1*$^{-/-}$ MEFs treated with 25 μM FCCP for 12 and 24 hrs. B) Quantification of COX IV protein levels (n=5, *p<0.05, ns = not significant). C) Representative images of WT and *Becn1*$^{-/-}$ MEFs overexpressing the mitophagy reporter and myc-Parkin, challenged with 10 μM FCCP for 12 hrs (scale bars = 10 nm). D) Quantification of red-only puncta after subtraction of yellow signal, expressed as number of mitophagy events per cell number (n=3, 30 cells/experiment imaged, **p<0.01, ns = not significant) (scale bar = 10 μm). Statistical test: One-way analysis of variance (ANOVA) followed by Tukey's multiple comparison test.

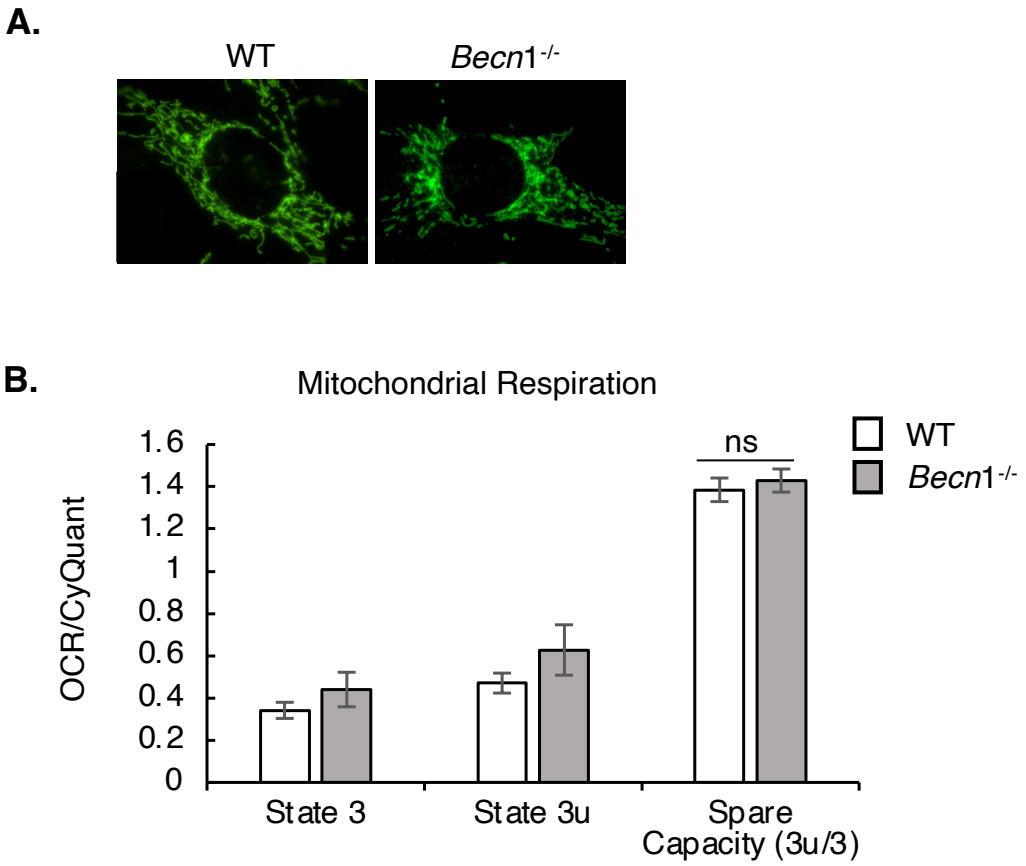

Figure 4.4 Mitochondrial respiration is functional in *Becn1*$^{-/-}$ MEFs. A) Representative immunofluorescent images of cells stained with Tom20 antibody to label mitochondria. B) Oxygen Consumption Rate in WT and *Becn1*$^{-/-}$ MEFs at different states of measurement. State 3 initiated with ADP, State 3u is FCCP-induced maximal uncoupler-stimulated respiration.

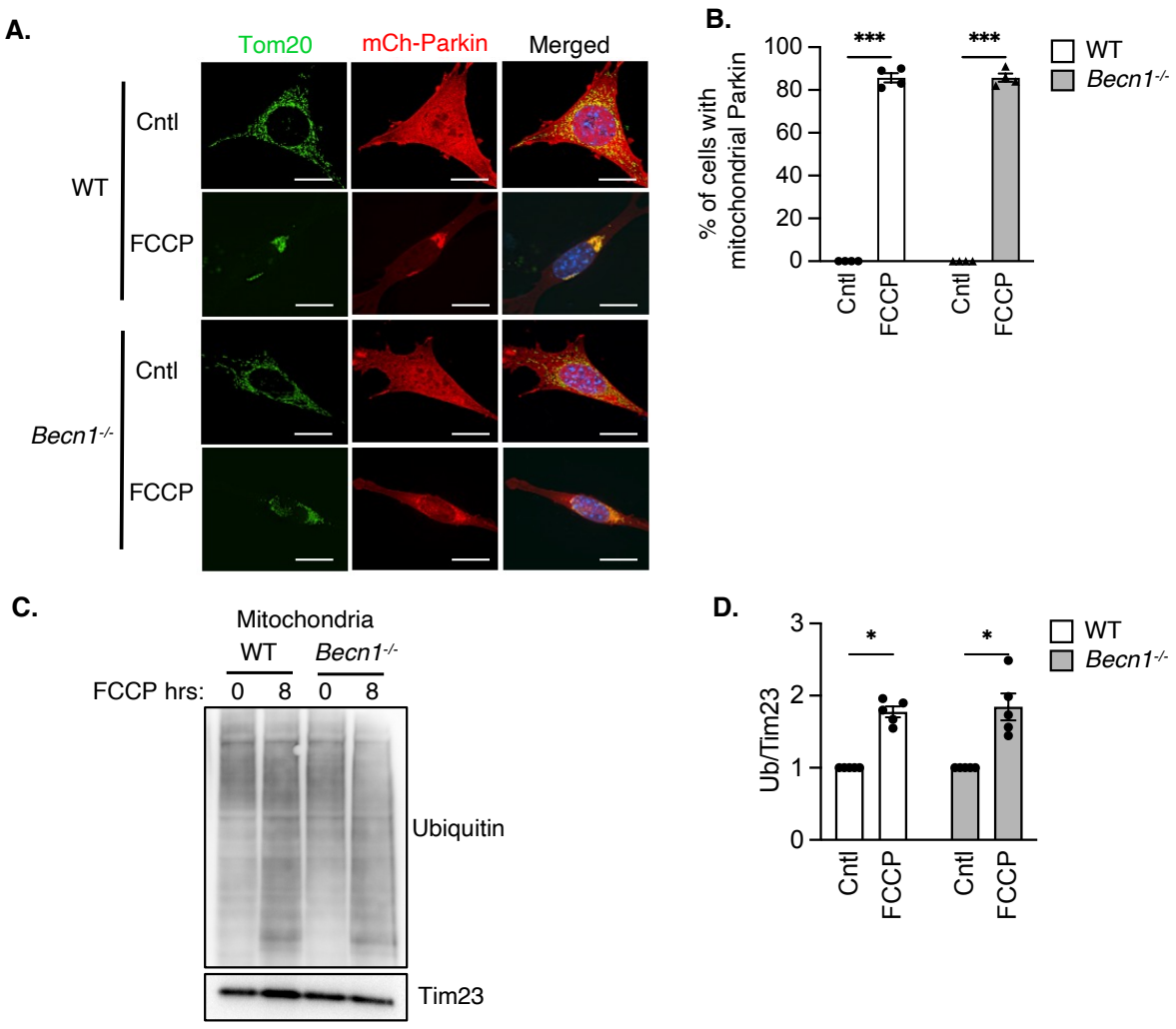

Figure 4.5 Parkin recruitment to depolarized mitochondria is intact in the absence of Beclin1. A) Representative images of WT and *Becn1*$^{-/-}$ MEFs overexpressing mCherry (mCh)-Parkin and stained for Tom20 after 6 hours of 10 μM FCCP treatment. Nuclei were counter stained with Hoechst (scale bars = 10 nm). B) Quantification of percent cells with Parkin at mitochondria (n=3, 100 cells/experiment, ***p<0.001). C) Representative Western blot of Ubiquitin levels in isolated mitochondrial fractions from WT and *Becn1*$^{-/-}$ MEFs treated with 10 μM FCCP. D) Quantification of protein levels (n=5, *p<0.05). Statistical test: One-way analysis of variance (ANOVA) followed by Tukey's multiple comparison test.

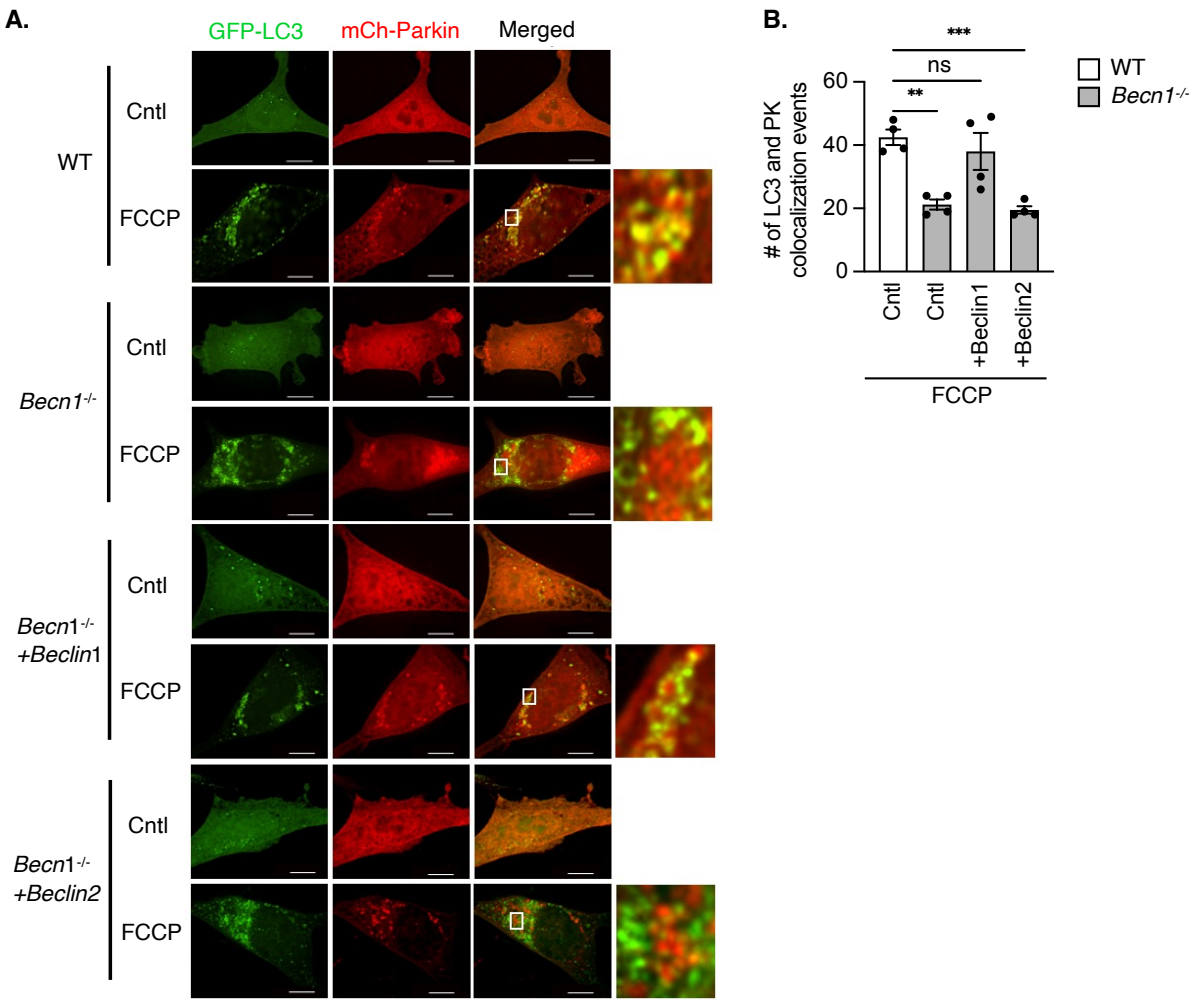

Figure 4.6 Beclin1-deficient MEFs have decreased targeting of autophagosomes to Parkin-labeled mitochondria. A) Representative images of WT and *Becn1*$^{-/-}$ MEFs overexpressing GFP-LC3 and mCh-Parkin. Cells were treated with 10 μM FCCP for 6 hours. Zoomed in regions are indicated by white boxes (scale bars = 10 μm). B) Quantification of GFP-LC3 and mCh-Parkin (PK) colocalization events (n=4, 30 cells/experiment, **p<0.01, ***p<0.001, ns = not significant). Statistical test: One-way analysis of variance (ANOVA) followed by Tukey's multiple comparison test.

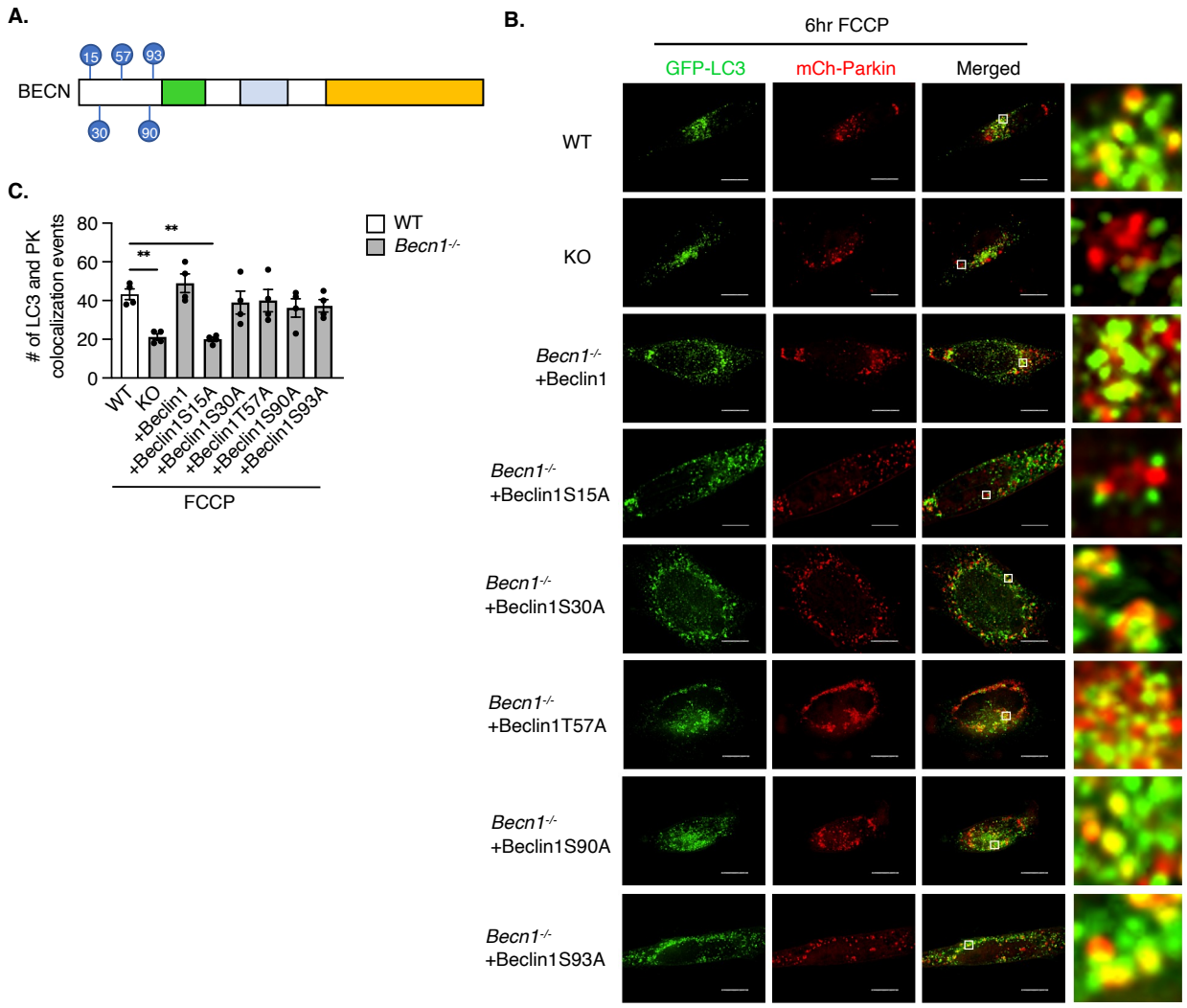

Figure 4.7 BeclinS15 phosphorylation site contributes to the proper targeting of autophagosomes to damaged mitochondria. A) Phosphorylation sites in Beclin1's N-terminus. B) Representative images of WT and *Becn1*$^{-/-}$ MEFs overexpressing GFP-LC3, mch-Parkin. Beclin1 or Beclin1 mutants. Cells were treated with 10 μM FCCP for 6 hours. Zoomed in regions are indicated by white boxes. B) Quantification of GFP-LC3 and mCh-Parkin colocalization events (n=3, 30 cells/experiment, **p<0.01) (scale bars = 10 μm). Statistical test: Two-way analysis of variance (ANOVA) followed by Tukey's multiple comparison test.

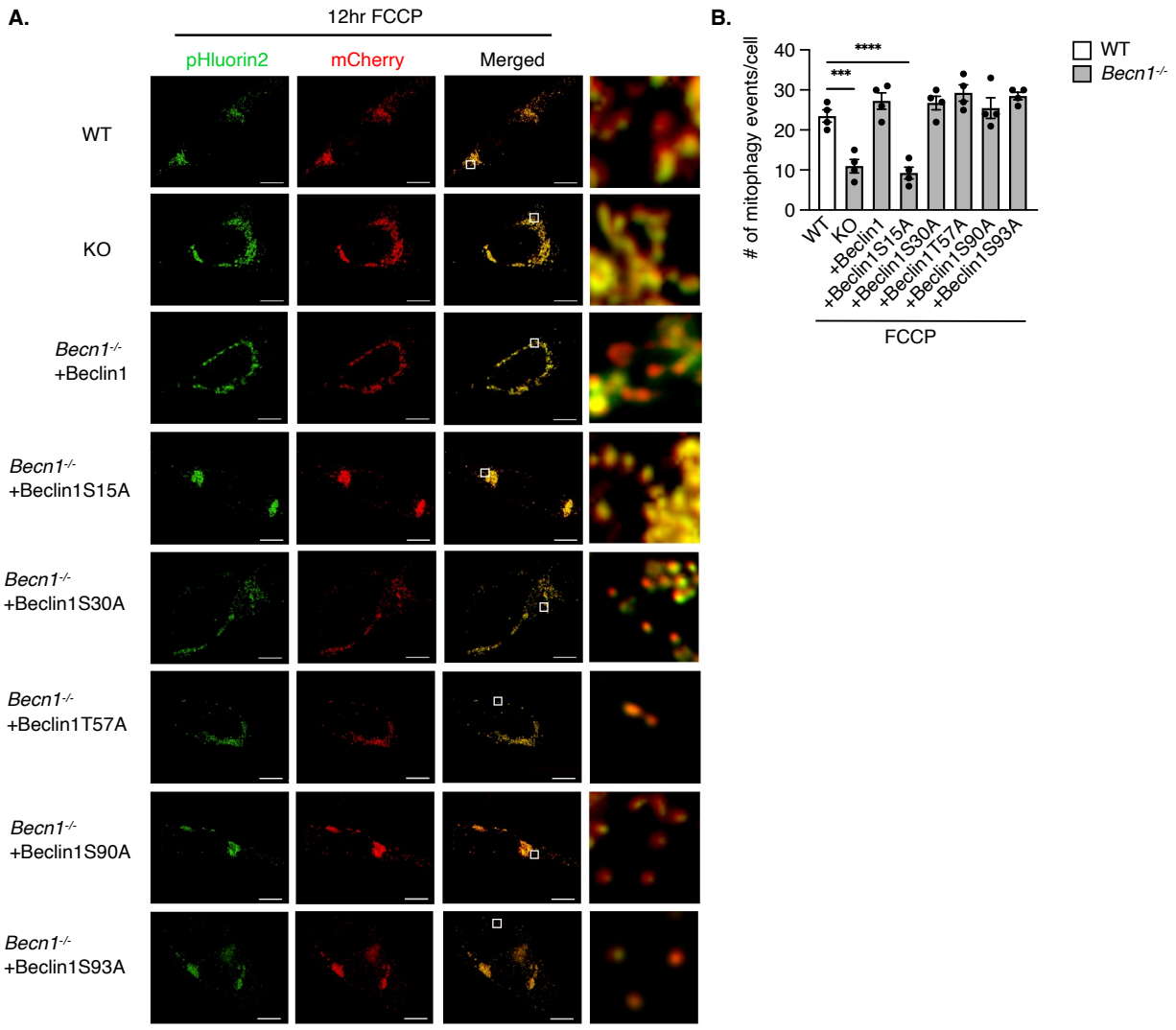

Figure 4.8 BeclinS15 phosphorylation site is important for effective clearance of damaged mitochondria. A) Representative images of WT and *Becn1*$^{-/-}$ MEFs overexpressing mitophagy reporter, myc-Parkin, and Beclin1 or Beclin1 mutants. Cells were treated with 10 μM FCCP for 12 hours. Zoomed in regions are indicated by white boxes (scale bars = 10 μm). B) Quantification of mitophagy events, as measured by number of red-only puncta after subtraction of yellow signal (n=3, 30 cells/experiment imaged, ***p<0.001, ****p<0.0001). Statistical test: Two-way analysis of variance (ANOVA) followed by Tukey's multiple comparison test.

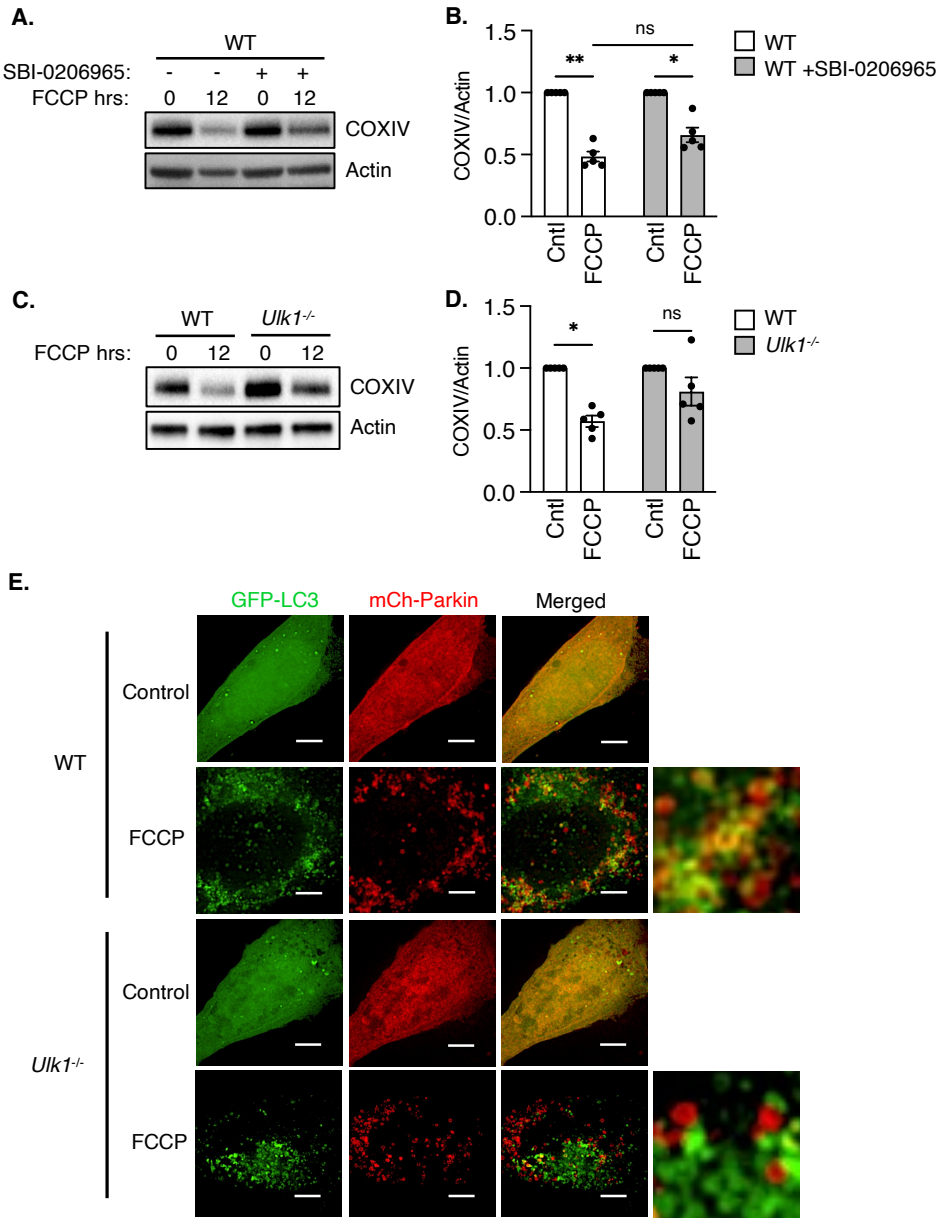

Figure 4.9 ULK1 is required for targeting of autophagosomes to mitochondria. A) Representative Western blot of COX IV levels in WT MEFs overexpressing flag-Parkin. Cells were treated with the ULK inhibitor SBI-0206965 (20 μM) plus FCCP (25 μM) for 12 hours. B) Quantification of COX IV protein levels (n=5, *p<0.05, **p<0.01). C) Representative Western blot of COX IV levels in WT and *Ulk1*$^{-/-}$ MEFs, overexpressing flag-Parkin, and treated with 25 μM FCCP (12h). D) Quantification of COX IV protein levels (n=5, *p<0.05, ns = not significant) E) Representative images of WT and *Ulk1*$^{-/-}$ MEFs overexpressing GFP-LC3 and mCh-Parkin treated with 10 μM FCCP for 6 hours (scale bars = 10 μm). Statistical test: Two-way analysis of variance (ANOVA) followed by Tukey's multiple comparison test.

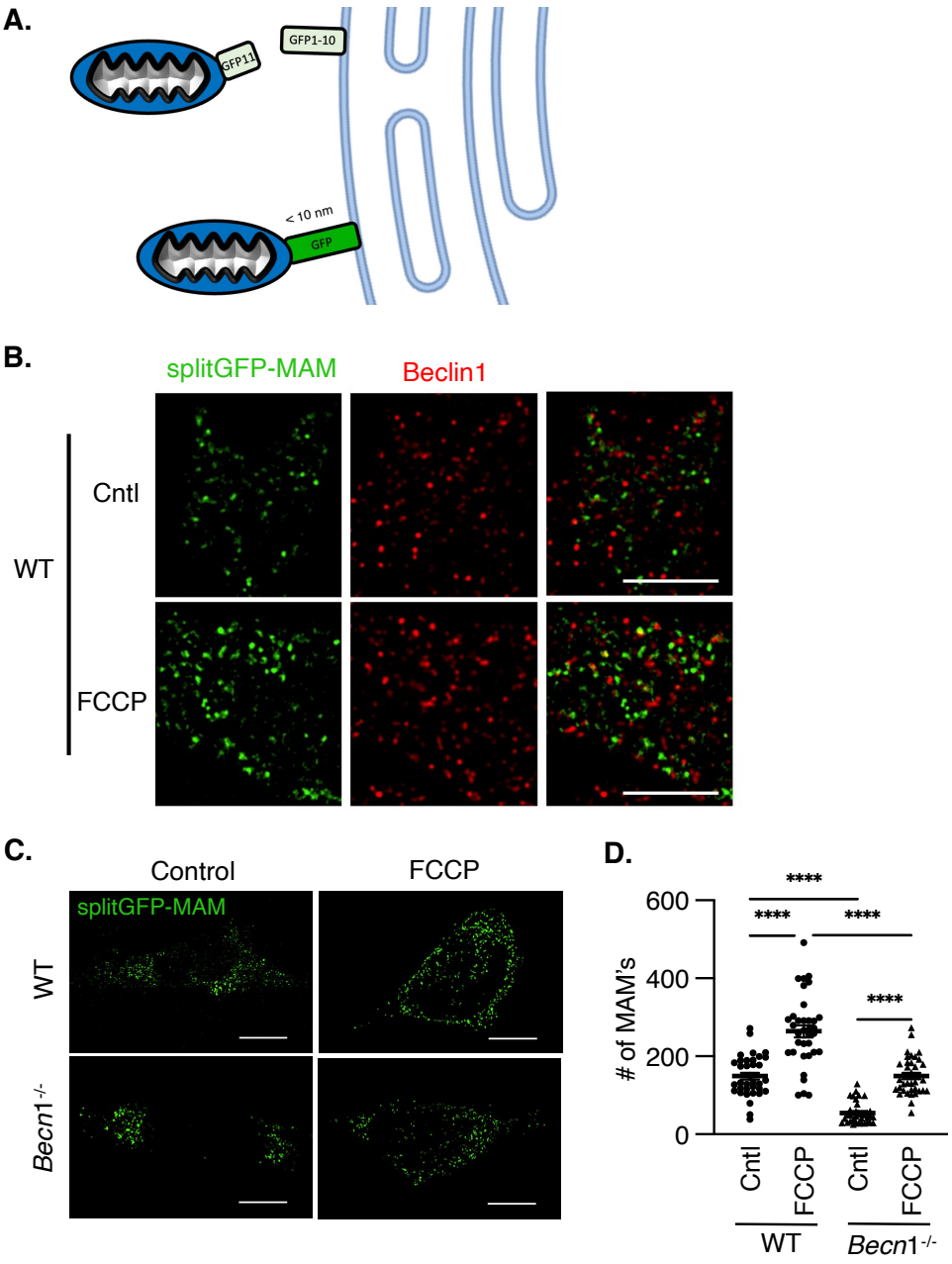

Figure 4.10 Beclin1 associates with mitochondrial-associated membranes. A) Schematic of the split-GFP-MAM reporter that fuses to form a full GFP when within 10 nm of each other. B) Representative images of WT MEFs overexpressing the split-GFP mitochondrial-associated membrane (MAM) reporter. Cells were stained for Beclin1 at baseline (cntl) and after treatment with 10 μM FCCP for 6 hours (scale bars = 5μm). C) Representative images of WT and *Becn1*$^{-/-}$ MEFs overexpressing a split-GFP MAM reporter before and after treatment with 10 μM FCCP for 6 hours (scale bars = 10 μm). D) Quantification of the number of MAMs/cell, plotted on a per cell basis (30 cells/experiment, ****p<0.0001). Statistical test: Ordinary one-way analysis of variance (ANOVA) followed by Tukey's multiple comparison test.

CHAPTER 5: Mitophagy Reporter

5.1 Introduction

Degradation of aged and damaged mitochondria by mitophagy is essential to maintain a healthy mitochondrial network. Quantification of mitophagy in tissues or cells can be achieved by various approaches, including Western blots and fluorescent imaging; however, a detailed and accurate understanding of this process requires researchers to be able to measure levels of mitophagy within individual cells. Furthermore, the ability to monitor mitophagy on a single-cell basis is essential to understanding how clearance of damaged mitochondria within one cell affects a total population.

Classical approaches to visually monitoring mitophagy, either by EM or by autophagosome and mitochondria colocalization, are limited and can be costly. However, the number of approaches to monitoring mitophagy within individual cells has greatly expanded in the past decade. A number of novel mitophagy reporters have recently been generated, including mt-Keima, mt-QC, and mt-Rosella, described in detail in the introduction to this thesis. Each of these reporters uses pH-sensitive fluorophores, that are altered by the low pH that occurs when a lysosome fuses with an autophagosome. Each of these reporters also targets their fluorescent tags specifically to the mitochondria.

These reporters have greatly expanded our ability to track and quantify mitophagy in individual cells; however, all the reporters come with certain limitations. For example, the mt-Keima reporter uses a fluorophore whose excitation spectra shifts in a pH-dependent manner. While effective, this method requires a specialized filter set and image processing, available in few labs. In contrast, while mt-QC and mt-Rosella both

use traditional red and green fluorophores, each has its own shortcomings. Firstly, using multiple emissions spectra limits the number of additional stains that can be performed. Furthermore, outer membrane proteins are targeted for degradation by the ubiquitin proteosome system (UPS) even during mitophagy, complicating the analysis of mt-QC. mt-Rosella uses the same mitochondrial-targeting peptide used in the mt-Keima reporter, COX VIII, which targets proteins to the mitochondrial matrix. However, mt-Rosella uses the red fluorophore DsRed, which our lab has found to be susceptible to aggregation.

We set out to engineer a new mitophagy reporter that avoids the problems with existing reporters. We systematically compared a variety of reporters using different combinations of fluorophores and mitochondrial targeting mechanisms to generate a highly efficient reporter. In this chapter, we will discuss our goals and criteria applied while making our own version of a mitophagy reporter, and how it has led to the generation of a cardiac transgenic mitophagy reporter mouse.

5.2 Results

To generate an improved mitophagy reporter, we considered two main factors: how to target the reporter to mitochondria and what fluorophores to use. To the best of our knowledge, no other groups have extensively compared and contrasted targeting options or fluorophores of mitophagy reporters. We generated several different constructs with different combinations of targeting sequences and fluorophores (Fig. 5.1).

For targeting the reporter to mitochondria, we considered three options: target the reporter to the mitochondrial matrix, anchor it to the outer mitochondrial membrane, or anchor it to the inner mitochondrial membrane in the matrix. Each of these targeting

strategies may come with potentially confounding effects on the function of the mitochondria or the efficacy of the reporter. Our first option was to target the reporter to the mitochondria using a simple mitochondrial targeting sequence (MTS). This sequence is present in mitochondrial proteins that are encoded by the nucleus to ensure proper localization. Upon delivery to the mitochondrial matrix, the MTS peptide is cleaved by mitochondrial proteases, trapping the protein inside the matrix (*Mitochondrial Targeting Signal - an Overview | ScienceDirect Topics*, n.d.). This approach was used by both mt-Keima and mt-Rosella reporters, which used the MTS from COX VIII. Therefore, these reporters are localized to the matrix without being anchored.

Our second option was to target the reporter to the outer mitochondrial membrane, similar to the mt-QC reporter. However as previously mentioned, outer membrane proteins are susceptible to degradation by the UPS (Neutzner et al., 2007). Our final option was to anchor the reporter to the inner mitochondrial membrane by attaching a transmembrane (TM) sequence to the reporter. We ruled out using the entire sequence of any mitochondrial protein to prevent issues of interference with expression. This would give us the certainty that any mitochondrial phenotype we observed in cells was due to the reporter's expression and not overexpression of a protein. Instead, we decided utilize the MTS from ATP synthase, to ensure localization to the mitochondrial matrix. We combined it with the TM domain sequence from the myeloid-cell leukemia 1 (Mcl-1) protein, to physically tie the reporter to the inner membrane.

The second factor was which fluorophores to use for the reporter. Similar to published reporters, we wanted to take advantage of the pH change upon autophagosome-lysosome fusion. However, our goal was to use fluorophores to

maximize signal to noise and specificity that could be visualized on a standard microscope. We ruled out using dual-excitation fluorophores based on the need for specialized microscope filters for the acquisition of mt-Keima. We decided the dependability in using two spectra, similar to mt-QC and mt-Rosella, would be more reliable, thus we utilized using a red spectra-associated fluorophore in combination with a green spectra-associated fluorophore. We considered multiple options in the red and green spectra and tried different combinations (Fig. 5.1).

When considering red spectra, we had many options. We initially narrowed our choices to dsRed, mCherry, and mCardinal based on the excitation/emission spectra, acid sensitivity, brightness, and overall reliability of these fluorophores. Although used in the mt-Rosella reporter, we ruled out dsRed as this fluorophore has high rates of aggregation when tagged to proteins. We decided to compare mCherry, based on its success in mt-QC and also on its acid sensitivity of 4.5 pH. We also compared it to mCardinal because its excitation/emission spectra are in far-red, potentially increasing the ability to perform additional staining in the red spectra.

When considering green spectra, we used 2 varieties of the pH-sensitive pHluorin fluorophore. pHluorin was developed to lose fluorescence as acidity increases, with loss of fluorescence starting at pH 6.5. The original pHluorin fluorophore had issues with overall brightness, placing a higher demand on the exposure time and light source power. pHluorin2 was generated to have an 8-fold enhanced brightness compared to pHluorin but retained the pH sensitivity.

We generated and screened several variants of mitophagy reporters. We set three clear criteria for the reporters to meet at baseline. 1. Correct targeting to mitochondria

without altering morphology; 2. Clear visualization of both fluorophores at baseline; 3. Pixel intensity from both red and green channels must be significantly above the background. Based on these criteria, we were able to eliminate MTS-mCherry-pHluorin due to a weak pHluorin signal that required high lamp power and exposure time during imaging. We further ruled out several reporters based on abnormal mitochondrial phenotypes that appeared regularly at baseline. Representative images of some of the issues encountered can be seen in Figure 5.2. Tom20-Phluorin-mCherry, displayed weak and nonspecific mitochondrial signal, while also having occasional green-only mitochondria, which should never be observed. MTS-mCardinal-pHluorin2 frequently had no mitochondria-localized signal but instead had bright nuclear expression of the fluorophores. Overexpression of MTS-mCardinal-pHluorin2-TM led to fragmentation of the mitochondrial network.

After progressive elimination of constructs according to our criteria, two constructs remained: MTS-mCherry-pHluorin2 and MTS-mCherry-pHluorin2-TM. Both of these reporter constructs localize to the matrix, but one of them is anchored in the inner membrane facing the matrix. In general, these two reporters behaved similarly and matched our initial criteria. However, in subsequent experiments, we caught occasional inconsistencies in the pHluorin2 colocalization with mCherry in the MTS-mCherry-pHluorin2 construct, and so we decided to proceed with MTS-mCherry-pHluorin2-TM.

The next step was to determine whether pHluorin fluorescence was quenched upon autophagosome-lysosome fusion. We co-stained cells carrying our construct with a LAMP2 antibody, to detect the lysosomal-associated membrane protein. Only cells

carrying MTS-mCherry-pHluorin2-TM had red-only puncta, reflecting reporters with green fluorescence quenched by acidification, engulfed by lysosomal membranes (Fig. 5.3).

5.3 Discussion

The investigation of mitophagy as a homeostatic cellular process and a potential source of dysregulation in disease requires reporters to track and quantify mitophagy *in vitro* and ultimately *in vivo*. Although several mitophagy reporters have been generated in recent years, all of them have limitations. We set out to engineer a novel reporter system, taking advantage of learned knowledge from existing reporters. To this end, systematically tested combinations of targeting mechanisms and fluorophores to ensure the production of the most efficient and accurate reporter possible.

From our original 7 reporter constructs, we found a single construct, MTS-mCherry-pHluorin2-TM, that met all our criteria for a mitophagy reporter. This included strong and specific fluorescent signals, performance under FCCP challenge, and accurate colocalization to mitochondria and the lysosome during mitophagy. This novel reporter features several key improvements over previously generated reporters. First, this reporter has higher sensitivity to acidity where pHluorin2 is quenched at pH 6.5 instead of GFP at pH 6.0 allowing for more sensitivity and earlier detection of autophagosome-lysosome fusion. It also has a brighter signal-to-noise ratio since pHluorin2 emits 8-fold higher than pHluorin. The mCherry fluorophore, in contrast to pHluorin2, is relatively resistant to pH change and will emit fluorescence after the pHluorin signal is quenched. mCherry is also a preferable fluorophore compared to dsRed, the fluorophore used in mt-Rosella, because dsRed is susceptible to aggregation. The

specific combination of pHluorin2 and mCherry should therefore allow for detection of early mitophagy events and for an extended period of time compared to GFP-based systems.

The novel use of targeting to the inner membrane also presents a potentially important advantage over previous reporters. mt-QC, for example, is targeted to the outer membrane of the mitochondria where it may be rapidly degraded by the proteosome in response to mitochondrial damage. Conversely, targeting to the mitochondrial matrix using the MTS, as was done in mt-Keima and mt-Rosella, may easier lead to the export of reporter proteins. Intriguingly, in these experiments, two nearly identical constructs, MTS-mCherry-pHluorin2 and MTS-mCherry-pHluorin2-TM behaved differently, with only the TM-linked reporter successfully reflecting lysosomal engulfment, as MTS-mCherry-pHluorin2 displayed inconsistencies in the pHluorin2 signal compared to mCherry.

Overall, the behavior of this new mitophagy reporter is very promising, both at baseline conditions and in response to stress. This new reporter has already been illuminating in experiments with mitophagy in the lab; the robustness and specificity of this reporter can be clearly seen in Chapter 4 of this dissertation. Based on the *in vitro* success of this reporter, we have generated a transgenic mouse line that specifically expresses this reporter in the heart (Fig. 5.4). As mitophagy is important in mitochondrial-rich tissues with a high metabolic load, we anticipate that this mouse model may provide insight both into the process of mitophagy in general and *in vivo* also into diseases that affect mitophagy.

5.4 Acknowledgments

Parts of Chapter 5 are in preparation for a manuscript for submission to a journal. Gonzalez, E. R., Jeung, R. H., Gustafsson, A. B. The primary author is the lead investigator and author of this manuscript.

Reporter	Mitochondrial Location	Green	Red
MTS-pHluorin1-mCherry	Matrix	pHluorin1	mCherry
Tom20-pHluorin1-mCherry	OMM	pHluorin1	mCherry
MTS-mCherry-pHLuorin2	Matrix	pHLuorin2	mCherry
MTS-mCherry-pHLuorin2-TM	IMM	pHLuorin2	mCherry
MTS-mCardinal-pHLuorin2	Matrix	pHLuorin2	mCardinal
MTS-mCardinal-pHLuorin2-TM	IMM	pHLuorin2	mCardinal

Figure 5.1 Variations of Mitophagy Reporters. Different mitophagy reporters generated and tested in cells.

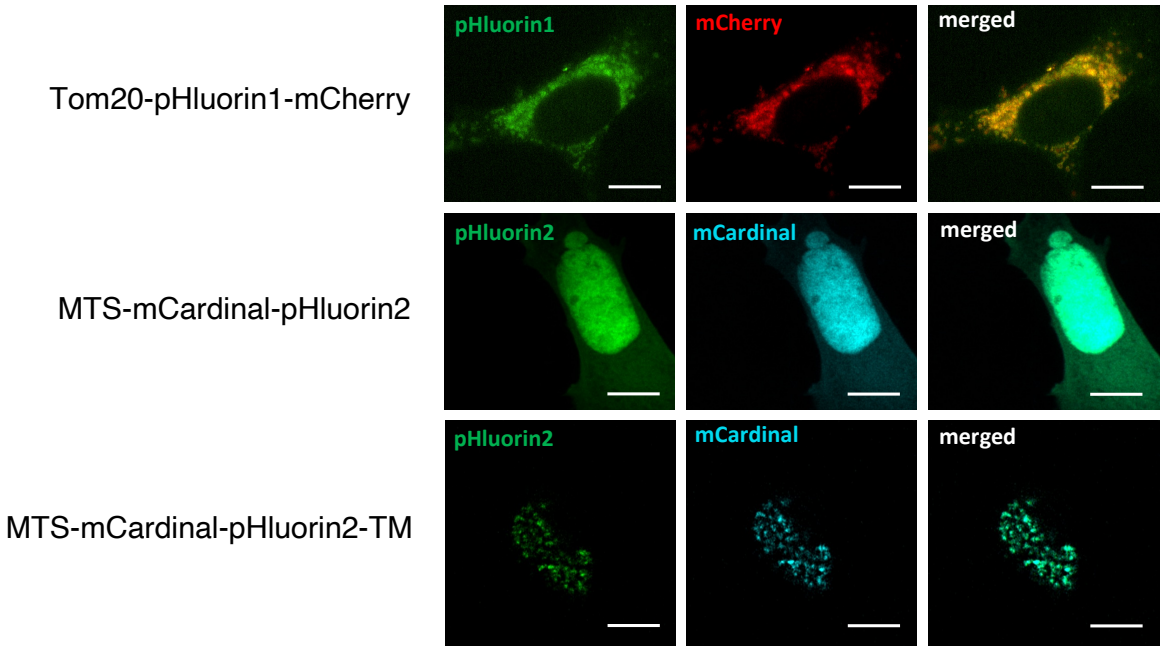

Figure 5.2 Common issues with various mitophagy reporters. Representative images of 3 key issues encountered with some of the mitophagy reporters. Tom20-Phluorin1-mCherry displayed weak fluorescence and mislocalization. MTS-mCardinal-pHluorin2 signal was often mislocalized to the nucleus. MTS-mCardinal-pHluorin2-TM generates a fragmented mitochondrial network at baseline. (scale bars = 10 μm).

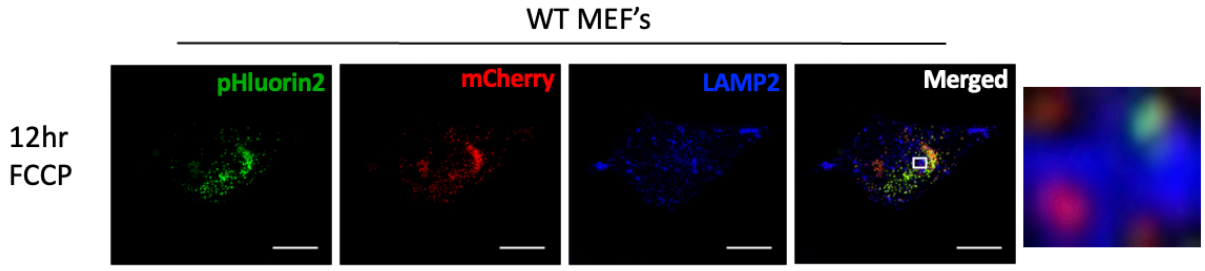

Figure 5.3 Red only mitochondria associate with LAMP2. The mitophagy reporter was overexpressed in WT MEFs treated with 10 μm FCCP for 12 hours. Cells were fixed and stained with Lysosome-associated membrane protein 2 (LAMP2) (scale bars = 10 μm).

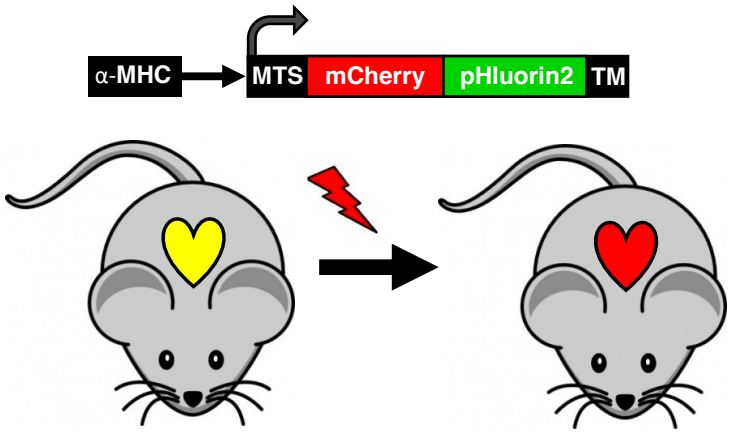

Figure 5.4 Generation of cardiac-specific Mitophagy Reporter Mice. We generated a transgenic mouse line overexpressing the mitophagy reporter under the α-MHC promoter to target our reporter to the heart. We will assess levels of mitophagy in heart tissue based on the presence of red only mitochondria.

CHAPTER 6: Discussion

6.1 Introduction

My dissertation addresses similarities and differences between Beclin1 and Beclin2 in autophagy and mitophagy. These studies have expanded the understanding of Beclin1 cell-specific differences in autophagy and began the exploration of potential compensation mechanisms with Beclin2. I also further dissected the involvement of Beclin1 in mitophagy in autophagosome targeting. Finally, I generated a new fluorescent tool that can report mitophagy events both *in vivo* and *in vitro*.

6.2 Beclin1 and Beclin2 in Autophagy

Beclin1 was discovered as an ortholog of the yeast protein Atg6 and identified as the first mammalian autophagy gene in 1998 (Yue et al., 2003). Since its discovery, Beclin1 has been widely studied in the context of autophagy and is considered a key component of two separate class III PI3K complexes involved in autophagy, one that initiates phagophore formation and one that aids in autophagosome maturation (Itakura et al. 2008). In 2013, a Beclin1 homolog, Beclin2, was discovered and observed to interact with similar binding partners to Beclin1 that are involved in the class III PI3K complex (He et al. 2013). Despite this, there have been no studies investigating the relationship between Beclin1 and Beclin2. In this study, I first demonstrate that neither Beclin1 nor Beclin2 are essential to autophagic activity, but a compensation mechanism between the two proteins may exist (Fig. 6.1A). Additionally, we provide evidence a Beeclin1-and-Beclin2-independent autophagy pathway exists (Fig. 6.1B). We also show that Beclin1 appears to have different roles in stress response depending on cell type and species.

Finally, our data suggest there may be different functional redundancy of Beclin proteins depending on cell origin and type, therefore affecting the activity of compensatory mechanisms.

In chapter 3, I show that neither Beclin1 nor Beclin2 are essential for autophagic flux in mouse or human cells. Although autophagosome formation was reduced, GFP-LC3 positive autophagosome structures did still successfully form in the absence of Beclin1 or Beclin2. Beclin-1 independent autophagy has been observed in breast cancer and hypoxia but the exact mechanisms are unknown (Scarlatti et al. 2008; Wu, Huang, and Lin 2014). Because Beclin1 and Beclin2 have been reported to interact with the same class III PI3K complexes, it lends to reason that Beclin2 dependent autophagy is what may actually be occurring (He et al. 2013). To explore this hypothesis, I next looked at autophagic activity in cells lacking both Beclin1 and Beclin2. The baseline rate of autophagic degradation appeared to be independent of Beclin1 and Beclin2 and therefore suggests that a Beclin1-and-Beclin2 independent mechanism of autophagosome formation exists in cells.

I also show that Beclin1 appears to have cell-type-specific roles in response to autophagy-inducing stress. MEFs were capable of generating a robust response to autophagy-inducing stimuli in the absence of Beclin1. HeLa cells, however, had significant impairment in their response. The difference between these two different cell lines exists not only in the species but also in cell type and further investigation is needed to dissect which factors influence Beclin1's roles.

Adding to the layer of cell type-specificity, our data in chapter 3 also suggests potentially different functional redundancy between mouse and human. We observe

increased *Becn2* expression in both mouse MEFs and human HeLa cells in response to stress. However, MEFs display intact autophagic activity in response to stress, while HeLa cells have an impaired response to FCCP, suggesting compensation mechanisms between Beclin1 and Beclin2 may be more efficient in mouse lines. The exact mechanisms of compensation for loss of Beclin1 or Beclin2 in each system require further investigation.

6.3 Beclin1 as a Regulator of Autophagosome Targeting in Mitophagy

Parkin-mediated mitophagy is an essential quality control process in maintaining mitochondrial and cellular homeostasis. Beclin1 has previously been implicated in mitophagy autophagosome formation at the MAMs, reportedly through its interaction with PINK1 (Gelmetti et al. 2017, 1). However, our study shows Ulk1 phosphorylation of Beclin1 on the Serine 15 residue promotes autophagosome targeting to damaged mitochondria. We demonstrate that Beclin1, and not Beclin2, is specific to mitophagy. We also show that the Serine 15 residue on Beclin1, targeted by Ulk1, contributes to autophagosome targeting. Lastly, we confirm and expand on Beclin1's association with MAMs.

In chapter 4, I show Beclin1, but not Beclin2 is specific to mitophagy. Using *BECN1*$^{-/-}$ and *BECN2*$^{-/-}$ HeLa cells, we only observed decreased rates of Parkin-mediated mitochondrial clearance in cells lacking Beclin1. We confirmed these observations in MEFs as well and found that decreased clearance was a result of impaired autophagosome targeting to cargo. Only overexpression of Beclin1, and not Beclin2, in *Becn1*$^{-/-}$ MEFs rescued autophagosome targeting to mitochondria. This is contrary to

observations made by the Levine group, where they implicated Beclin2 plays a role in mitophagy (He et al. 2013).

We also provide evidence that Serine 15 in Beclin1 is targeted by Ulk1 and contributes to the targeting of autophagosomes to mitochondria. Although it was previously established that Serine 15 was a target residue of Ulk1, the contribution of autophagosome targeting was not. Studies established the Serine 15 site as a regulator in VPS34 complex activation and autophagosome induction (Russell et al. 2013; Park et al. 2018). We validated Ulk1's specificity to this site's influence using a Ulk1 inhibitor. Evaluation of several known phosphorylation sites in the unique N-terminal region of Beclin1 only revealed Serine 15 to be important in mitophagy. With this data, we have established a new purpose for Ulk1 phosphorylation of Serine15.

Finally, we presented data that supports previous observations of Beclin1 association with MAMs (Gelmetti et al. 2017). We expanded on this with the use of a splitGFP-MAM reporter and observation of a total number of MAMs within an individual cell. Interestingly, we observed a decreased baseline number of MAMs in the absence of Beclin1. Although, the number of MAMs still increased in response to mitochondrial stress, the offset compared to WT numbers was still prominent.

Together, these findings implicate a new role for Beclin1, as a site of phosphorylation for Ulk1 to promote the targeting of autophagosomes at the MAMs (Fig. 6.2).

6.4 Fluorescent Reporters

Tools to study mitophagy both *in vivo* and *in vitro* are very limited. In the past decade, there has been a heavy emphasis on the importance of visualizing mitophagy events within individual cells. At present, there are several popular mitophagy reporters in use, but each has severe methodological limitations either in the fixation, imaging, or targeting steps. We tried to circumvent some of those issues by designing a new mitophagy reporter in a systematic way, detailed in Chapter 6.

We generated and screened several different mitophagy reporters, made from combinations of different targeting sequences and fluorophores. In this chapter, we detail our methodological approach to vetting these variants of mitophagy reporters' variants and how we ruled out many options using our set criteria. The data in chapter 6 provides representative images of common issues encountered with many of our mitophagy reporter variants, which will be a valuable resource to the community of mitophagy researchers.

We ultimately selected the MTS-mCherry-pHluorin2-TM reporter based on its fluorescent intensity, reporting sensitivity, and accuracy. The successful and effective use of the reporter in our study of Beclin1 in mitophagy (Chapter 5) drove our decision to develop a cardiac-specific transgenic mouse expressing our reporter.

6.5 Relevance

Overall, this foundational work has greatly contributed to our understanding of Beclin1 and Beclin2 biology. The compensatory mechanisms suggested by these studies underscore the importance of the robust maintenance of autophagy in cells. Furthermore,

the cell-specific behavior of Beclin1 that we identified, reminds us that extreme caution should be used in extrapolating results from other systems.

6.6 Future Directions

One future direction that pertains to my work in chapter 3 would be to investigate Beclin1-and-Beclin2 independent autophagy pathways, implicated in our experiments with cells lacking both Beclin1 and Beclin2. Autophagy defects have been implicated in a variety of diseases. A better understanding of the mechanisms by which cells compensate for the lack of Beclin1 and or Beclin2 to maintain autophagic activity could reveal new therapeutic targets.

Another important future direction would be to investigate the role of Beclin2 *in vivo.* Only one study has characterized Beclin2 *in vivo* and implied Beclin2 plays a role in mitophagy. Therefore, there should be additional focus on characterizing this protein to create a more robust framework of Beclin2's functions.

To further expand on our observations of mitophagy, it is essential to dissect the direct influence of Ulk1 in targeting Beclin1 to the MAMs. We are actively evaluating our Beclin1 Serine 15 phospho-mutants localization and associated with MAMs before and after stress. Additionally, we are also studying Ulk1's influence on Beclin1 targeting to MAMs with a Ulk1 inhibitor.

Additionally, the study of Beclin1 relevance in mitophagy could be greatly expanded upon by crossing Beclin1$^{+/-}$ mice with our cardiac-specific mitophagy reporter transgenic mice. We would be able to evaluate changes in mitophagy activity at baseline and also in response to pathophysiological challenges, such as myocardial infarction.

Combining *in vivo* data with our *in vitro* findings of Beclin1 in mitophagy could provide a greater degree of evidence that Beclin1 regulates autophagosome targeting to damaged mitochondria.

6. 7 Concluding Remarks

The work done in this dissertation contributes to the growing knowledge of Beclin1 and Beclin2 in the processes of autophagy and mitophagy. Additionally, the creation of a new mitophagy reporter for use *in vivo* and *in vitro* is a widely applicable tool for the mitophagy research community. These findings promote the evolution of our understanding of these vital cellular processes and provide a scaffold for future investigations.

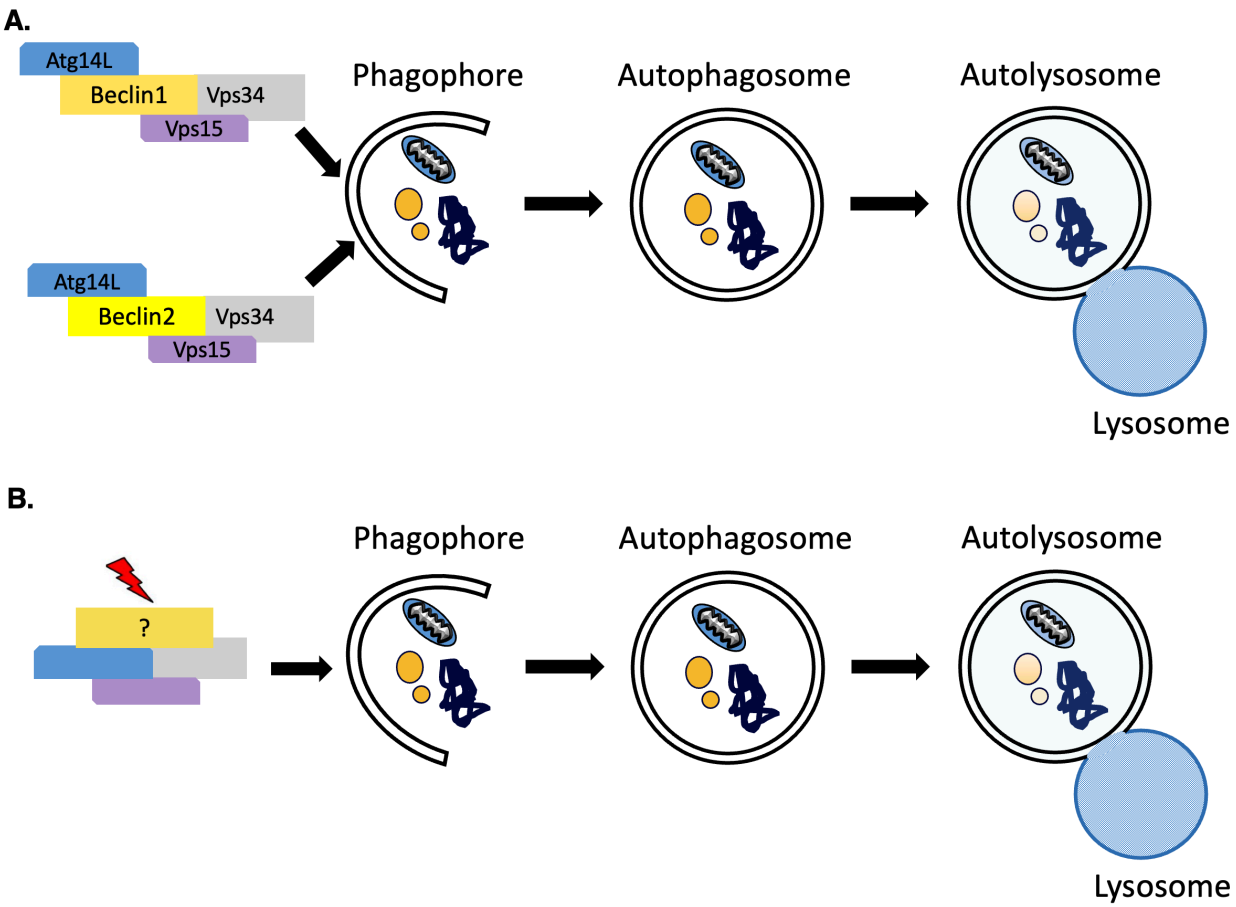

Figure 6.1 A) Our model of compensation between Beclin1 and Beclin2 in autophagosome formation at baseline. B) Our model of a Beclin1-and-Beclin2-independent mechanism involved in autophagosome formation during stress.

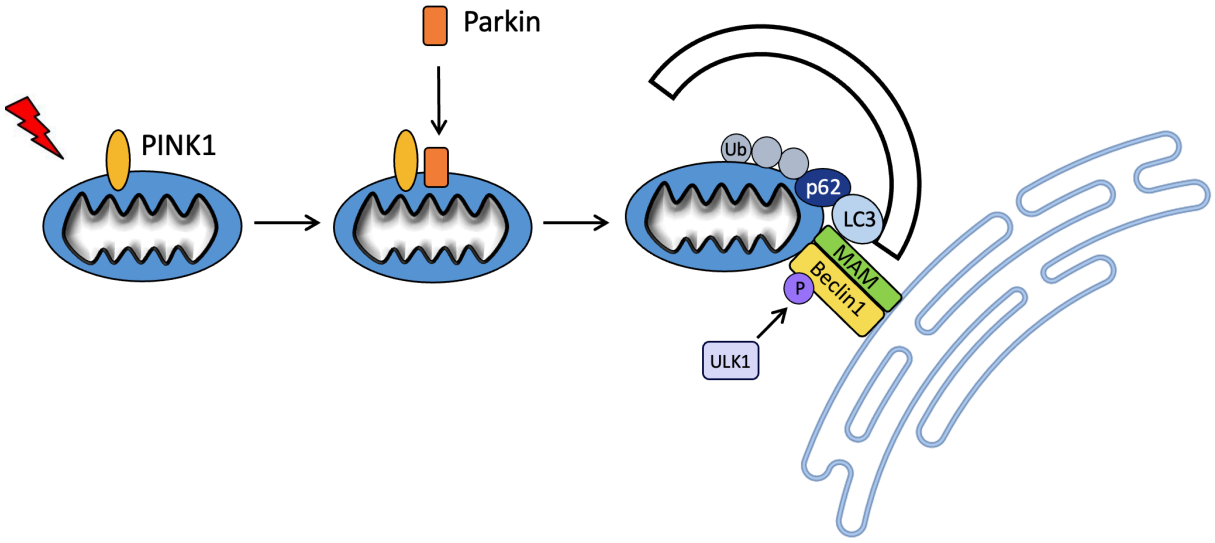

Figure 6.2 Model of Beclin1 association with MAMs to promote autophagosome localization to damaged mitochondria after phosphorylation by Ulk1.

References

Calì, T., Ottolini, D., Vicario, M., Catoni, C., Vallese, F., Cieri, D., Barazzuol, L., & Brini, M. (2019). SplitGFP Technology Reveals Dose-Dependent ER-Mitochondria Interface Modulation by α-Synuclein A53T and A30P Mutants. *Cells*, *8*(9), E1072. https://doi.org/10.3390/cells8091072

Cieri, D., Vicario, M., Giacomello, M., Vallese, F., Filadi, R., Wagner, T., Pozzan, T., Pizzo, P., Scorrano, L., Brini, M., & Calì, T. (2018). SPLICS: A split green fluorescent protein-based contact site sensor for narrow and wide heterotypic organelle juxtaposition. *Cell Death and Differentiation*, *25*(6), 1131–1145. https://doi.org/10.1038/s41418-017-0033-z

Dikic, I., & Elazar, Z. (2018). Mechanism and medical implications of mammalian autophagy. *Nature Reviews. Molecular Cell Biology*, *19*(6), 349–364. https://doi.org/10.1038/s41580-018-0003-4

Gelmetti, V., De Rosa, P., Torosantucci, L., Marini, E. S., Romagnoli, A., Di Rienzo, M., Arena, G., Vignone, D., Fimia, G. M., & Valente, E. M. (2017). PINK1 and BECN1 relocalize at mitochondria-associated membranes during mitophagy and promote ER-mitochondria tethering and autophagosome formation. *Autophagy*, *13*(4), 654–669. https://doi.org/10.1080/15548627.2016.1277309

Guo, J. Y., Teng, X., Laddha, S. V., Ma, S., Van Nostrand, S. C., Yang, Y., Khor, S., Chan, C. S., Rabinowitz, J. D., & White, E. (2016). Autophagy provides metabolic substrates to maintain energy charge and nucleotide pools in Ras-driven lung cancer cells. *Genes & Development*, *30*(15), 1704–1717. https://doi.org/10.1101/gad.283416.116

Hamasaki, M., Furuta, N., Matsuda, A., Nezu, A., Yamamoto, A., Fujita, N., Oomori, H., Noda, T., Haraguchi, T., Hiraoka, Y., Amano, A., & Yoshimori, T. (2013). Autophagosomes form at ER-mitochondria contact sites. *Nature*, *495*(7441), 389–393. https://doi.org/10.1038/nature11910

He, C., Wei, Y., Sun, K., Li, B., Dong, X., Zou, Z., Liu, Y., Kinch, L. N., Khan, S., Sinha, S., Xavier, R. J., Grishin, N. V., Xiao, G., Eskelinen, E.-L., Scherer, P. E., Whistler, J. L., & Levine, B. (2013). Beclin 2 functions in autophagy, degradation of G protein-coupled receptors, and metabolism. *Cell*, *154*(5), 1085–1099. https://doi.org/10.1016/j.cell.2013.07.035

Itakura, E., Kishi, C., Inoue, K., & Mizushima, N. (2008). Beclin 1 forms two distinct phosphatidylinositol 3-kinase complexes with mammalian Atg14 and UVRAG. *Molecular Biology of the Cell*, *19*(12), 5360–5372. https://doi.org/10.1091/mbc.e08-01-0080

Kakimoto, Y., Tashiro, S., Kojima, R., Morozumi, Y., Endo, T., & Tamura, Y. (2018). Visualizing multiple inter-organelle contact sites using the organelle-targeted

split-GFP system. *Scientific Reports*, *8*(1), 6175. https://doi.org/10.1038/s41598-018-24466-0

Liang, C., Lee, J., Inn, K., Gack, M. U., Li, Q., Roberts, E. A., Vergne, I., Deretic, V., Feng, P., Akazawa, C., & Jung, J. U. (2008). Beclin1-binding UVRAG targets the class C Vps complex to coordinate autophagosome maturation and endocytic trafficking. *Nature Cell Biology*, *10*(7), 776–787. https://doi.org/10.1038/ncb1740

Lin, M. G., & Hurley, J. H. (2016). Structure and function of the ULK1 complex in autophagy. *Current Opinion in Cell Biology*, *39*, 61–68. https://doi.org/10.1016/j.ceb.2016.02.010

Mahon, M. J. (2011). pHluorin2: An enhanced, ratiometric, pH-sensitive green florescent protein. *Advances in Bioscience and Biotechnology (Print)*, *2*(3), 132–137. https://doi.org/10.4236/abb.2011.23021

Maiuri, M. C., Criollo, A., Tasdemir, E., Vicencio, J. M., Tajeddine, N., Hickman, J. A., Geneste, O., & Kroemer, G. (2007). BH3-Only Proteins and BH3 Mimetics Induce Autophagy by Competitively Disrupting the Interaction between Beclin 1 and Bcl-2/Bcl-XL. *Autophagy*, *3*(4), 374–376. https://doi.org/10.4161/auto.4237

Matsui, Y., Takagi, H., Qu, X., Abdellatif, M., Sakoda, H., Asano, T., Levine, B., & Sadoshima, J. (2007). Distinct roles of autophagy in the heart during ischemia and reperfusion: Roles of AMP-activated protein kinase and Beclin 1 in mediating autophagy. *Circulation Research*, *100*(6), 914–922. https://doi.org/10.1161/01.RES.0000261924.76669.36

McKnight, N. C., Zhong, Y., Wold, M. S., Gong, S., Phillips, G. R., Dou, Z., Zhao, Y., Heintz, N., Zong, W.-X., & Yue, Z. (2014). Beclin 1 is required for neuron viability and regulates endosome pathways via the UVRAG-VPS34 complex. *PLoS Genetics*, *10*(10), e1004626. https://doi.org/10.1371/journal.pgen.1004626

McWilliams, T. G., Prescott, A. R., Allen, G. F. G., Tamjar, J., Munson, M. J., Thomson, C., Muqit, M. M. K., & Ganley, I. G. (2016). Mito-QC illuminates mitophagy and mitochondrial architecture in vivo. *The Journal of Cell Biology*, *214*(3), 333–345. https://doi.org/10.1083/jcb.201603039

Menon, M. B., & Dhamija, S. (2018). Beclin 1 Phosphorylation—At the Center of Autophagy Regulation. *Frontiers in Cell and Developmental Biology*, *6*, 137. https://doi.org/10.3389/fcell.2018.00137

Mercer, T. J., Ohashi, Y., Boeing, S., Jefferies, H. B. J., De Tito, S., Flynn, H., Tremel, S., Zhang, W., Wirth, M., Frith, D., Snijders, A. P., Williams, R. L., & Tooze, S. A. (2021). Phosphoproteomic identification of ULK substrates reveals VPS15-dependent ULK/VPS34 interplay in the regulation of autophagy. *The EMBO Journal*, *40*(14), e105985. https://doi.org/10.15252/embj.2020105985

Narendra, D. P., Jin, S. M., Tanaka, A., Suen, D.-F., Gautier, C. A., Shen, J., Cookson, M. R., & Youle, R. J. (2010). PINK1 is selectively stabilized on impaired mitochondria to activate Parkin. *PLoS Biology*, *8*(1), e1000298. https://doi.org/10.1371/journal.pbio.1000298

Pickles, S., Vigié, P., & Youle, R. J. (2018). Mitophagy and Quality Control Mechanisms in Mitochondrial Maintenance. *Current Biology: CB*, *28*(4), R170–R185. https://doi.org/10.1016/j.cub.2018.01.004

Pickrell, A. M., & Youle, R. J. (2015). The Roles of PINK1, Parkin, and Mitochondrial Fidelity in Parkinson's Disease. *Neuron*, *85*(2), 257–273. https://doi.org/10.1016/j.neuron.2014.12.007

Rubinsztein, D. C., Shpilka, T., & Elazar, Z. (2012). Mechanisms of autophagosome biogenesis. *Current Biology: CB*, *22*(1), R29-34. https://doi.org/10.1016/j.cub.2011.11.034

Russell, R. C., Tian, Y., Yuan, H., Park, H. W., Chang, Y.-Y., Kim, J., Kim, H., Neufeld, T. P., Dillin, A., & Guan, K.-L. (2013). ULK1 induces autophagy by phosphorylating Beclin-1 and activating VPS34 lipid kinase. *Nature Cell Biology*, *15*(7), 741–750. https://doi.org/10.1038/ncb2757

Schneider, C. A., Rasband, W. S., & Eliceiri, K. W. (2012). NIH Image to ImageJ: 25 years of image analysis. *Nature Methods*, *9*(7), 671–675. https://doi.org/10.1038/nmeth.2089

Sun, Y., Yao, X., Zhang, Q.-J., Zhu, M., Liu, Z.-P., Ci, B., Xie, Y., Carlson, D., Rothermel, B. A., Sun, Y., Levine, B., Hill, J. A., Wolf, S. E., Minei, J. P., & Zang, Q. S. (2018). Beclin-1-Dependent Autophagy Protects the Heart During Sepsis. *Circulation*, *138*(20), 2247–2262. https://doi.org/10.1161/CIRCULATIONAHA.117.032821

Tian, W., Li, W., Chen, Y., Yan, Z., Huang, X., Zhuang, H., Zhong, W., Chen, Y., Wu, W., Lin, C., Chen, H., Hou, X., Zhang, L., Sui, S., Zhao, B., Hu, Z., Li, L., & Feng, D. (2015). Phosphorylation of ULK1 by AMPK regulates translocation of ULK1 to mitochondria and mitophagy. *FEBS Letters*, *589*(15), 1847–1854. https://doi.org/10.1016/j.febslet.2015.05.020

Yue, Z., Jin, S., Yang, C., Levine, A. J., & Heintz, N. (2003). Beclin 1, an autophagy gene essential for early embryonic development, is a haploinsufficient tumor suppressor. *Proceedings of the National Academy of Sciences of the United States of America*, *100*(25), 15077–15082. https://doi.org/10.1073/pnas.2436255100

Zhu, H., Tannous, P., Johnstone, J. L., Kong, Y., Shelton, J. M., Richardson, J. A., Le, V., Levine, B., Rothermel, B. A., & Hill, J. A. (2007). Cardiac autophagy is a

maladaptive response to hemodynamic stress. *Journal of Clinical Investigation*, *117*(7), 1782–1793. https://doi.org/10.1172/JCI27523